Downregulation of HOXA3 in lung adenocarcinoma and its relevant molecular mechanism analysed by RT-qPCR, TCGA and *in silico* analysis

BIN-LIANG GAN[1*], RONG-QUAN HE[1*], YU ZHANG[2], DAN-MING WEI[2], XIAO-HUA HU[1] and GANG CHEN[2]

Departments of [1]Medical Oncology, and [2]Pathology, First Affiliated Hospital of Guangxi Medical University, Nanning, Guangxi Zhuang Autonomous Region 530021, P.R. China

Abstract. Recent studies have indicated that homeobox A3 (*HOXA3*) functions as a carcinogen in colon cancer and the methylation level of *HOXA3* is significantly increased in lung adenocarcinoma (LUAD) tissues. However, at least to the best of our knowledge, few studies to date have been performed on *HOXA3* in non-small cell lung cancer (NSCLC). Therefore, further studies on *HOXA3* expression in NSCLC and the potential regulatory mechanisms are urgently required. In this study, *HOXA3* expression in 55 tissues of cases of NSCLC and corresponding non-lung cancer tissues was detected by reverse transcription-quantitative PCR (RT-qPCR). In addition, the clinical significance of *HOXA3* expression in NSCLC was evaluated using the Cancer Genome Atlas (TCGA) database. Bioinformatics analysis was then performed to elucidate the potential molecular mechanisms of action of *HOXA3*. Furthermore, the potential target microRNAs (miRNAs or miRs) of *HOXA3* were predicted using miRWalk2.0. Based on Gene Expression Omnibus (GEO) and TGCA databases, standardized mean difference (SMD) and sROC methods were used for meta-analyses of the expression of potential target miRNAs of *HOXA3* in NSCLC to evaluate their association with *HOXA3*. The results revealed that the *HOXA3* expression levels in NSCLC, LUAD and lung squamous cell carcinoma (LUSC) were 0.1130±0.1398, 0.1295±0.16890 and 0.0906±0.0846, respectively. These values were all decreased compared with the normal tissues (0.1877±0.1975, 0.2337±0.2405 and 0.1249±0.0873, respectively, P<0.05). The TCGA database also revealed the low expression trend of *HOXA3*. The downregulation of *HOXA3* may play an important role in the progression and the poor prognosis of LUAD. The TCGA database also suggested that *HOXA3* in LUAD and LUSC tissues exhibited certain mutational levels. In addition, the methylation levels in the NSCLC, LUAD and LUSC tissues significantly increased [NSCLC: fold change (FC), 1.3226; P<0.001; LUAD: FC, 1.2712; P<0.001; and LUSC: FC, 1.3786; P<0.001]. According to the analyses using the Kyoto Encyclopedia of Genes and Genomes (KEGG), we found that the co-expression *HOXA3* genes were mainly associated with the focal adhesion signalling pathway and the ECM-receptor interaction signalling pathway. Furthermore, the predicted miRNA, miR-372-3p, exhibited a high expression in both the NSCLC and LUAD tissues (P<0.05). On the whole, the findings of this study indicate that low *HOXA3* expression may play a certain role in LUAD; however, its association with LUSC still requires further investigation. *HOXA3* function may be achieved through different pathways or target miRNAs. However, the specific underlying mechanisms need to be confirmed through various functional studies.

Correspondence to: Dr Dan-Ming Wei, Department of Pathology, First Affiliated Hospital of Guangxi Medical University, 6 Shuangyong Road, Nanning, Guangxi Zhuang Autonomous Region 530021, P.R. China
E-mail: danmingwei08@163.com

Dr Xiao-Hua Hu, Department of Medical Oncology, First Affiliated Hospital of Guangxi Medical University, 6 Shuangyong Road, Nanning, Guangxi Zhuang Autonomous Region 530021, P.R. China
E-mail: gxmuhxh@163.com

*Contributed equally

Introduction

The most recent data indicate that lung cancer remains the type of cancer with the highest prevalence among men and women and is also one of the most common causes of cancer-related mortality (1). Approximately 1.82 million cases of lung cancer are newly diagnosed globally each year, and approximately 1.37 million individuals succumb to the disease (2-4). Based on the histological classification, lung cancers are divided into 2 types: Non-small cancer lung cancer (NSCLC) and small cell lung cancer (SCLC). NSCLC accounts for 85% of all lung cancer cases (5). NSCLS includes a number of histological subtypes, including lung adenocarcinoma (LUAD), lung squamous cell carcinoma (LUSC) and large cell carcinoma (LCC). LUAD is one of the main subtypes of NSCLC (6). Despite
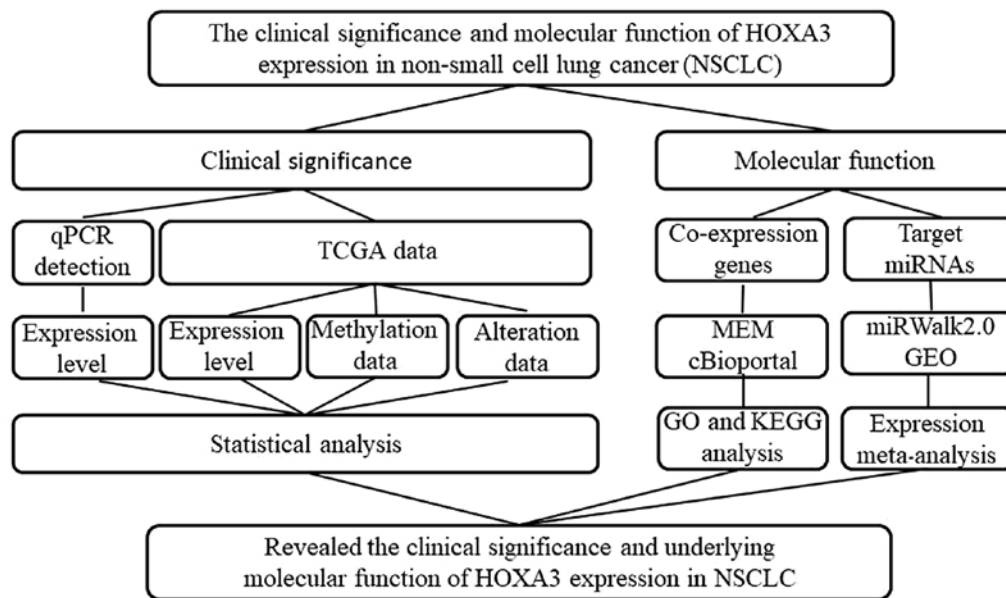
Figure 1. Flow chart of the study design of this study.

in-depth studies and significant progress being made in lung cancer treatment in recent decades (7-10), comprehensive clinical evaluation and in-depth molecular mechanistic studies are still required. Therefore, further investigations of the pathological mechanisms of NSCLC are warranted. Thus, the screening of novel functional genes and targets in NSCLC may provide basic data and a preliminary theoretic basis for further studies on the pathogenesis of NSCLC.

The homeobox (*HOX*) gene family is composed of 39 genes. These genes play critical roles in normal embryonic development by encoding transcription factors. The *HOX* gene family is divided into 4 groups: *HOXA*, *HOXB*, *HOXC* and *HOXD*. These genes localize to different chromosomal regions. The human *HOXA* gene cluster localizes to chromosome 7. There are 12 genes, including *HOXA1* to *HOXA11* and *HOXA13* (11-13). The *HOXA* gene cluster plays important roles in colorectal cancer, leukaemia, pancreatic cancer, oral squamous cell carcinoma and lung cancer (14-18). For *HOXA3*, only one study suggests that it nat be used as a biomarker of LUAD. This study was conducted by Daugaard *et al* (19). These researchers used a DNA methylation microarray to compare the genome-wide methylation patterns between tumour and tumour-adjacent lung tissues from 4 patients with LUAD and identified 74 differential methylation regions (DMRs). Through methylation sensitive-high resolution melting (MS-HRM) analyses, 18 DMRs were selected for validation in 52 LUAD tissues and 32 cancer-adjacent lung tissues. Finally, this study confirmed and validated 15 DMRs, including *HOXA3*, that could be used as biomarkers of LUAD (19). However, studies on the clinical significance and regulatory mechanisms of *HOXA3* expression in NSCLC are still lacking. Therefore, further studies are urgently required to examine *HOXA3* expression in NSCLC and to investigate the potential regulatory mechanisms in order to provide new insight into the pathogenic mechanisms of NSCLC.

In this study, we used reverse transcription-quantitative PCR (RT-qPCR) to detect *HOXA3* expression in NSCLC and normal lung tissues. *HOXA3* expression in NSCLC was validated using the Gene Expression Profiling Interactive Analysis (GEPIA) database. In addition, informatics analysis methods, including Gene Ontology (GO), Kyoto Encyclopedia of Genes and Genomes (KEGG) and protein-protein interaction (PPI), were performed to investigate the potential molecular mechanisms of action of *HOXA3*. Furthermore, the potential target microRNAs (miRNAs or miRs) of *HOXA3* were predicted using miRWalk2.0. The expression levels of miRNAs were validated using the Gene Expression Omnibus (GEO) and the Cancer Genome Atlas (TGCA) databases. The study design is presented in Fig. 1.

Materials and methods

Clinical samples. A total of 55 tissues of cases of clinical NSCLC and cancer-adjacent lung tissues were collected (from January, 2012 to February, 2014) at the Department of Pathology of The First Affiliated Hospital of Guangxi Medical University (Nanning, China). Among these 55 patients, 32 cases were diagnosed with LUAD, and 23 cases were diagnosed with LUSC. There were 41 men and 14 women. Patients were 23-90 years of age with a mean age of 56.9 years. Among these 55 cases, tumours in 39 cases were larger than 3 cm. Table I summarizes the detailed clinicopathological data of all the patients. Samples were fixed in formalin and embedded in paraffin. This research programme was approved by the Ethics Committee of the First Affiliated Hospital of Guangxi Medical University. All participants signed informed consent forms. All samples were diagnosed by 2 pathologists (G.C. and D.-M.W.) independently using the double-blind method.

Detection of HOXA3 expression by RT-qPCR. *HOXA3* expression in NSCLC samples was detected by RT-qPCR which was performed as previously described (20-22). Total RNA was extracted from the tumour and cancer-adjacent normal tissues using the RNeasy reagent (Qiagen, Shanghai, China). The RNA

Table I. The association of between HOXA3 mRNA expression in NSCLC tissues and patient clinicopathological characteristics based on RT-qPCR detection.

Clinicopathological characteristics	Case no.	HOXA3 expression			t-test of data	
		Mean	SD	FC	t-test	P-value
Group						
Control	55	0.19	0.20	1.00	2.86	0.006
Cancer	55	0.11	0.14	0.60		
Pathological type						
Adenocarcinoma	32	0.13	0.17	1.00	0.99	0.326
Squamous cell carcinoma	23	0.09	0.08	0.70		
LUAD						
Control	32	0.23	0.24	1.00	-1.94	0.023
Cancer	32	0.13	0.17	0.55		
LUAD						
Non-smoker	18	0.18	0.20	1.00	2.42	0.025
Smoker	14	0.06	0.04	0.32		
LUSC						
Control	23	0.12	0.09	1.00	-1.32	0.034
Cancer	23	0.09	0.08	0.73		
Sex						
Male	41	0.12	0.15	1.00	0.35	0.732
Female	14	0.10	0.12	0.87		
Age (years)						
<60	35	0.12	0.15	1.00	0.25	0.801
≥60	20	0.11	0.12	0.91		
Smoking						
No	30	0.14	0.17	1.00	1.91	0.064
Yes	25	0.08	0.06	0.54		
Size						
≤3 cm	16	0.12	0.12	1.00	0.09	0.931
>3 cm	39	0.11	0.15	0.97		
LNM						
No	29	0.08	0.10	1.00	-1.66	0.103
Yes	26	0.14	0.17	1.78		
TNM						
I-II	29	0.09	0.11	1.00	-1.26	0.212
III-IV	26	0.14	0.17	1.54		
Vascular invasion						
No	50	0.11	0.15	1.00	0.23	0.817
Yes	5	0.10	0.03	0.85		
Clinical grading						
I	5	0.09	0.08			0.664
II	40	0.12	0.16			
III	10	0.08	0.07			

HOXA3, homeobox A3, an mRNA of homeobox genes of clusters A; NSCLC, non-small cell lung cancer; LUAD, lung adenocarcinoma; LUSC, lung squamous cell carcinoma; RT-qPCR, reverse transcription-quantitative polymerase chain reaction; SD, standard deviation; FC, fold change; LNM, lymph node metastasis. An independent sample t-test was adopted to test the data and single factor ANOVA was used to test the clinical grading data. The difference between the cancer and normal adjacent group was analyzed by a paired-samples t-test.

concentration was measured using NanoDrop2000 (Thermo Fisher Scientific, Wilmington, DE, USA). Total RNA was reverse transcribed (10 μl reaction system) using a reverse transcription kit (ABI, Life Technologies, Carlsbad, CA, USA) to obtain cDNA for RT-qPCR. SYBR-Green (Shanghai GeneCore BioTechnologies Co., Ltd., Shanghai, China) was used to perform RT-qPCR and the distinctiveness of the PCR product was differentiated based on melting curve (23-26). RT-qPCR was carried out using the following conditions: preheating for 10 min at temprature 95˚C; and then repeating 40 cycles in temperature 95˚C for 15 sec and 60 sec at 60˚C. The primer sequences of *HOXA3* were as follows: Upstream, TCATTTAAGAGCGCCTGGACA and downstream primer, GAGCTGTCGTAGTAGGTCGC. Using *GAPDH* as an internal reference gene and the primer sequence were as follows: Upstream, 5'-TGGTCCCTGCTCCTCTAAC-3', downstream primer, 5'-GGCTCAATGGCGTACTCTC-3'. The relative expression level of *HOXA3* in this study was calculated using the $2^{-\Delta\Delta Cq}$ (27) formula (28, 29).

Retrieval of TCGA data. GEPIA (http://gepia.cancer-pku.cn/) is a visualization website based on TCGA data and contains differential gene expression between cancer and non-cancer, and analysis of the association between gene expression and overall survival (OS) or disease-free survival (DFS) and clinical stages (Stage). Survival analyses were performed using the log-rank test (also known as Mantel-Cox test) for hypothesis tests and calculation of the hazard ratio (HR) and 95% confidence interval (95% CI). Keywords, such as '*HOXA3*', 'LUAD' and 'LUSC', were searched in GEPIA to retrieve data of the differential expression of *HOXA3* in NSCLS, LUAD, LUSC and normal lung tissues, as well as information regarding the association between *HOXA3* and clinical stages and prognostic survival.

The keywords 'lung' and '*HOXA3*' were searched in the cBioPortal (http://www.cbioportal.org/) website to retrieve genetic alteration data of *HOXA3* in LUAD and LUSC. Data were obtained from microarray detection and RNA sequencing. In addition, DNA methylation data in LUAD and LUSC were downloaded from the Cancer Genome Atlas (TCGA: https://cancergenome.nih.gov/abouttcga/overview) database. *HOXA3* methylation data in LUAD and LUSC were screened.

HOXA3 co-expression genes. To investigate the intrinsic mechanisms of *HOXA3* expression in NSCLC tissues, we acquired *HOXA3*-associated co-expression genes from the MEM (http://biit.cs.ut.ee/mem) and cBioPortal databases. In MEM, when the score/P-value was smaller, the association between that gene and *HOXA3* was more significant. The results of 2 gene probes were extracted from MEM based on a P-value <0.0001, and the results were used for intersection. On the other hand, Pearson's correlation analysis was performed in cBioPortal to calculate the correlation between co-expression genes and *HOXA3*. When the absolute value of the Pearson's correlation coefficient was larger, the correlation was stronger. This study selected genes with an absolute value of the Pearsons' correlation coefficient >0.3 in NSCLC, LUAD and LUSC. Finally, the intersection results between MEM and cBioPortal were obtained and used for further analyses.

The overlapping genes were confirmed using a Venn diagram (http://bioinformatics.psb.ugent.be/webtools/Venn/).

Bioinformatics analyses. In this study, we used bioinformatics analyses to preliminarily investigate the molecular mechanisms of action of *HOXA3* in NSCLC. The final overlapping genes in MEM and cBioPortal were used for GO and KEGG analyses in David v6.7 (http://david.abcc.ncifcrf.gov/) to elucidate the enrichment of genes in biological processes and signalling pathways. PPI analyses were performed in STRING v10.5 (https://string-db.org/cgi/input.pl?input_page_show_search=on&UserId=HJJhhN v8hYyf&sessionId=Ce1Dx9pYDluc) to validate the protein interaction association to hypothesize the pathways through which *HOXA3* carries out its functions in NSCLC. The construction of the functional network was performed using Cytoscape 3.5.0 software and ClueGO plugin.

Prediction and preliminary validation of target miRNAs of HOXA3. The prediction of target miRNAs of *HOXA3* was performed in miRWalk2.0 (http://zmf.umm.uni-heidelberg.de/apps/zmf/mirwalk2/). miRWalk2.0 contains 12 on-line target gene prediction tools: Pictar2, miRWalk, miRMap, DIANA microT v4, PITA, miRanda, RNA22, mirBridge, miRDB, RNAhybrid, miRNAMap and TargetScan. miRNAs that were present in >8 software results were used as candidate miRNAs for further analyses.

The microarray results of differentially expressed miRNAs in lung cancer were searched in the GEO database and downloaded. The following search formula was employed: (lung OR pulmonary OR respiratory OR bronchi OR bronchioles OR alveoli OR pneumocytes OR 'air way') AND (cancer OR carcinoma OR tumor OR neoplas* OR malignan* OR adeno-carcinoma) AND (microRNA OR miRNA OR 'micro RNA' OR 'small temporal RNA' OR 'noncoding RNA' OR ncRNA OR 'small RNA'). We included microarray data containing expression data of miRNAs in lung cancer tissues and normal lung tissues and a sample number >3 into this study. Microarray data that did not conform to this condition were excluded. In addition, miRNA expression data for the LUAD, LUSC and normal lung tissues were extracted from the TCGA database. The mean value ± standard deviation (means ± SD) of the expression of potential target miRNAs in tumour and non-tumour tissues in each microarray was calculated. The random effects model was used to calculate the standardized mean difference (SMD) in STATA 2.0 software to evaluate the expression trend of miRNAs in NSCLC and plot the forest plot. In addition, analyses using the sROC method were performed to further validate the expression trend of miRNAs in NSCLC.

Statistical analyses. Statistical analyses of the experimental data were performed using SPSS 22.0 software (IBM, New York, NY, USA). The *HOXA3* expression levels detected by RT-qPCR were expressed as the means ± SD and the Mann-Whitney test was used to determine significance. The normal distribution was determined using the single-sample K-S test. The comparison of the association between the *HOXA3* expression level and the patient clinicopathological characteristics, and the comparison of mean values of 2 factors were performed using the independent sample t-test when variances were homogeneous. When variances
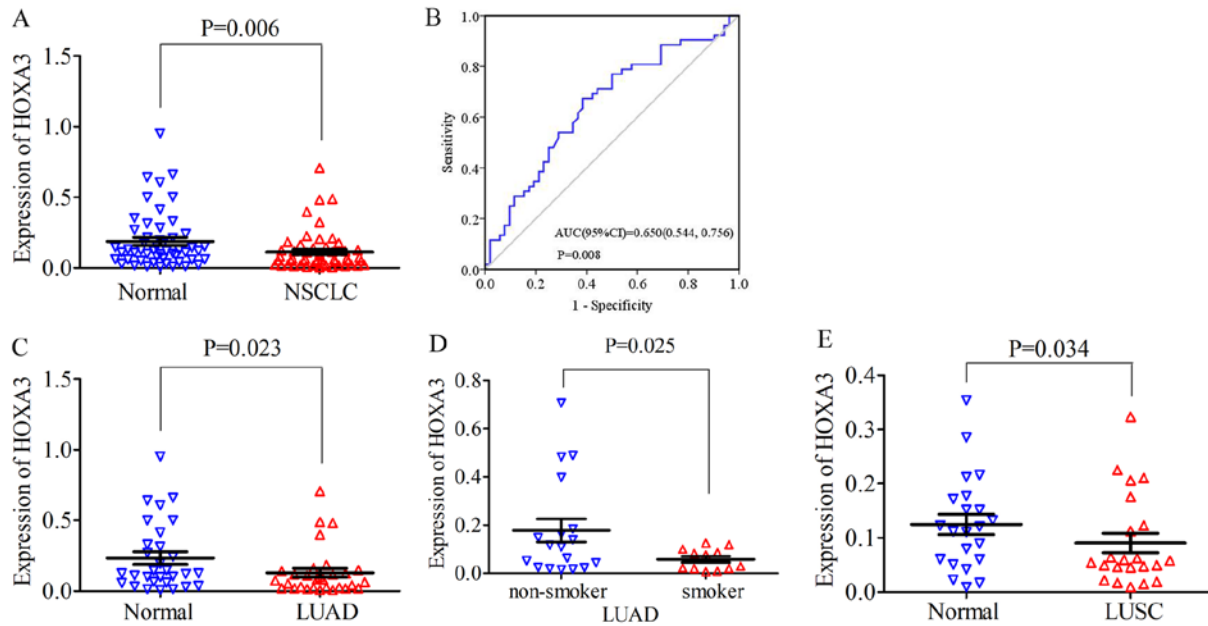
Figure 2. (A) Scatter diagram of HOXA3 expression between NSCLC tissue and normal lung tissue detected by RT-qPCR. (B) ROC curve of HOXA3 expression in NSCLC tissue. (C and D) Scatter plots of HOXA3 level in LUAD detected by RT-qPCR. (C) Differences between cancer and non-cancer. (D) Differences between smoker and non-smoker in LUAD. (E) HOXA3 expression between LUSC tissue and normal lung tissue detected by RT-qPCR. HOXA3, homeobox A3; NSCLC, non-small cell lung cancer; LUAD, lung adenocarcinoma; LUSC, lung squamous cell carcinoma.

were not homogeneous, rank sum statistical analysis was performed. The comparison of the mean values of multiple factors was performed using one-way analysis of variance (ANOVA) followed by the Bonferroni post hoc test, with a default P-value of 0.05. The differences in *HOXA3* expression levels between the NSCLC and normal lung tissues were further validated using the calculation of the area under the ROC curve. The Kaplan-Meier curve method was performed to analyse the association between the *HOXA3* expression level and NSCLC patient survival. Pearson's correlation analysis was used to calculate the correlation between two genes. GraphPad Prism was used to generate the scatter plot. Meta-analysis of target miRNAs in NSCLC and normal lung tissues was performed using the STATA 12.0 software. $P<0.05$ in all analytic results indicated that the differences exhibited statistical significance.

Results

HOXA3 expression in NSCLC. For NSCLC, the *HOXA3* expression level in the cancer tissues was 0.11±0.14 and the fold change (FC), 0.60 (FC is the fold change of *HOXA3* expression in tumour and non-tumour adjacent tissue). Compared with the normal lung tissues (0.19±0.20, P=0.006), *HOXA3* expression was significantly decreased (P=0.006; Fig. 2A). The median of the *HOXA3* level was 0.06 and the FC, 0.5 (control, 0.12; P=0.008). The area under the ROC curve (AUC) of low *HOXA3* expression in NSCLC was 0.65 (95% CI: 0.54, 0.76; P=0.008, Fig. 2B). Therefore, a low *HOXA3* expression may have some value in the occurrence of NSCLC. A low *HOXA3* expression was not significantly associated with the clinicopathological characteristics (Table I). In addition, in LUAD, the mean expression level of *HOXA3* was 0.13±0.17 and the FC, 0.55. *HOXA3* expression was

significantly decreased in LUAD compared with the cancer-adjacent normal tissues (0.24±0.24, P=0.023) (Fig. 2C and Table I). The median of the *HOXA3* level was 0.08 and the FC, 0.62 (control, 0.13; P=0.034). The AUC of downregulated *HOXA3* expression in LUAD was 0.66 (95% CI: 0.52, 0.80; P=0.035) (data not shown). Further analyses revealed that the *HOXA3* level in smokers (0.06±0.04) was reduced compared with that in non-smokers (0.186±0.20, P=0.025) (Fig. 2D and Table I). The AUC of downregulated *HOXA3* in the smoking group was 0.70 (95% CI: 0.51, 0.89; P=0.069) (data not shown). The combination of the above-mentioned data analyses demonstrated that the downregulation of *HOXA3* expression in LUAD was significant. In addition, *HOXA3* expression in LUAD may be associated with smoking, but did not exhibit a significant association with other clinicopathological characteristics. The analyses of the LUSC group alone revealed that *HOXA3* expression differed significantly between the cancer tissues and non-cancer tissues (cancer, 0.09±0.08 vs. control, 0.12±0.09, P=0.034, FC, 0.72) (Fig. 2E and Table I). The median of the *HOXA3* level was 0.06 and the FC, 0.5 (control, 0.12; P=0.113). The AUC of the low *HOXA3* level in the LUSC group was 0.64 (95% CI: 0.47, 0.81; P=0.113) (data not shown). The low expression of HOX3A in LUSC was not significantly associated with disease progression.

In addition, the GEPIA data revealed that *HOXA3* expression in LUAD (483 cases) was also significantly decreased compared with the normal lung tissues (347 cases) and exhibited a low expression trend in LUSC (LUSC, 486 cases; normal, 338 cases) (Fig. 3A). These results were consistent with the results of RT-qPCR. However, the association between the *HOXA3* expression level and the pathological stage did not exhibit an obvious pattern (Fig. 3B). We also acquired information regarding the association between the *HOXA3* expression level and the survival of patients with NSCLC, LUAD and
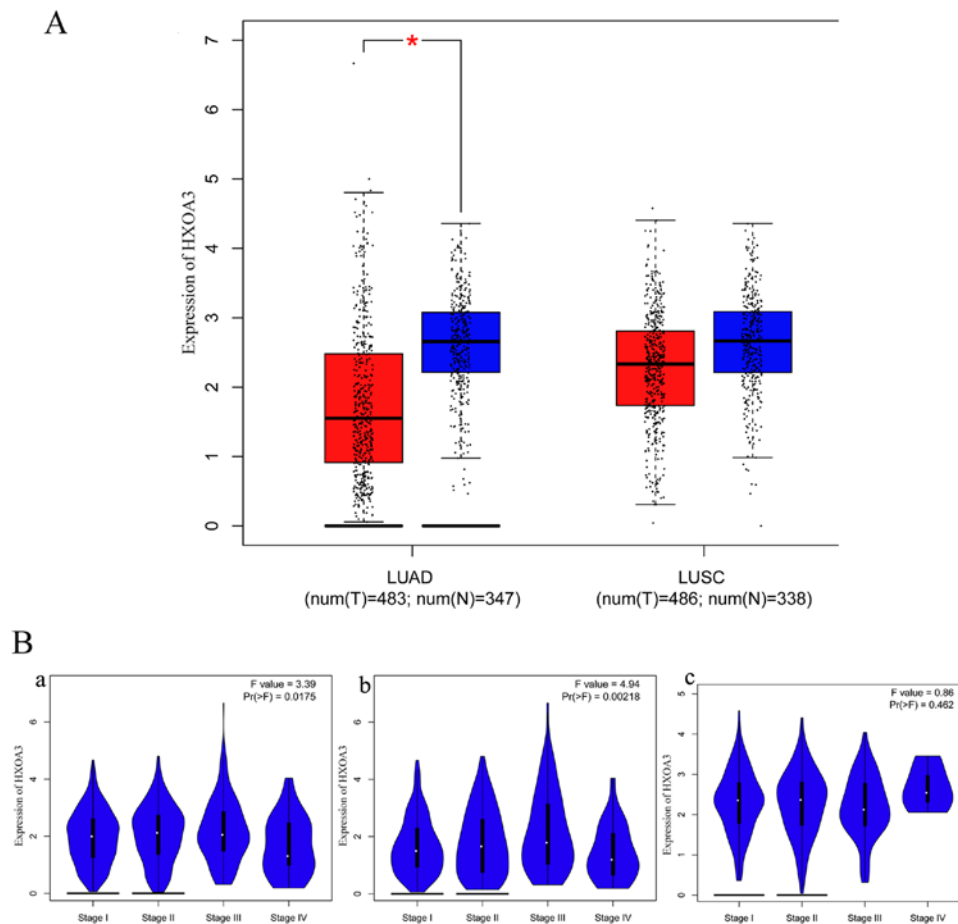
Figure 3. (A) Boxplot of HOXA3 expression in LUAD tissues vs. non-cancerous tissues and LUSC tissues vs. non-cancerous tissues; *P<0.05. (B) Pathological stage plot of HOXA3 levels in NSCLC. Panel a, NSCLC; panel b, LUAD; panel c, LUSC. HOXA3, homeobox A3; NSCLC, non-small cell lung cancer; LUAD, lung adenocarcinoma; LUSC, lung squamous cell carcinoma.

LUSC. Patients with NSCLC with a low *HOXA3* expression exhibited a better OS [HR (high), 1.3; P=0.0035] (Fig. 4A, panel a). Thus, a low *HOXA3* expression may be a protective factor of OS in patients with NSCLC. However, further analysis demonstrated that *HOXA3* was not significantly associated with the DFS of patients with NSCLC (Fig. 4A, panel d). The analyses of OS in the LUAD group alone demonstrated that patients with a high *HOXA3* expression exhibited an HR of 1.4 (P=0.042) (Fig. 4A, panel b), suggesting that a high *HOXA3* level may be a risk factor for the prognosis of LUAD. However, the *HOXA3* expression levels did not exhibit obvious predictive values as regards the DFS of patients with LUAD (Fig. 4A, panel e). In addition, the association between *HOXA3* and the prognosis of patients LUSC was not statistically significant (Fig. 4A, panels c and f), and this may require further investigation.

Furthermore, based on the microarray and RNA sequencing technologies, the sequencing results of 520 patients with LUAD revealed that the genetic alteration rates of *HOXA3* were 5% (24/520) and 11% (59/520). In addition, the sequencing results of 504 patients LUSC suggested that the genetic alteration rates of *HOXA3* were 5% (25/504), 7% (35/504) and 4% (18/504). Although the genetic alternation rates obtained using different methods differed, the final results all confirmed that *HOXA3* harboured genetic alterations in the LUAD and LUSC populations (Fig. 4B).

On the other hand, the methylation level of HOXA3 in the NSCLC tissues was 0.57±0.21 (FC, 1.32; P<0.001; Fig. 5A), with an AUC value of 0.72 (95% CI: 0.68, 0.76; P<0.001, Fig. 5D). The methylation level in the LUAD tissues was 0.56±0.20 (FC, 1.27; P<0.001; Fig. 5B), and an AUC value of 0.70 (95% CI: 0.64, 0.76; P<0.001, Fig. 5E). The methylation level in the LUSC tissues was 0.58±0.21 (FC, 1.38; P<0.001; Fig. 5C), and the AUC value was 0.74 (95% CI: 0.68, 0.79; P<0.001, Fig. 5F) (Table II). Compared with the normal tissues (NSCLC, 0.43±0.11; LUAD, 0.44±0.11; LUSC, 0.42±0.11), these levels were all significantly upregulated.

HOXA3 co-expression genes. Based on MEM, 11,488 and 4,730 *HOXA3* co-expression mRNA genes detected by 2 independent gene probes were obtained. The intersection between the results of 2 gene probes was collected, and a total of 1,709 more convincing co-expression mRNA genes were extracted. The data from cBioPortal revealed 3,600 and 2,676 co-expression mRNA genes in the NSCLC group and the LUAD group, respectively. Finally, the search results of the NSCLC group and the LUAD group in MEM and cBioPortal were processed using the crossing method (data not shown). In total, 293 and 213 genes were obtained, respectively, for further analysis.

Bioinformatics analyses. GO and KEGG analyses were performed on 293 and 213 genes in DAVID, and PPI network analyses were performed in STRING. The results from GO
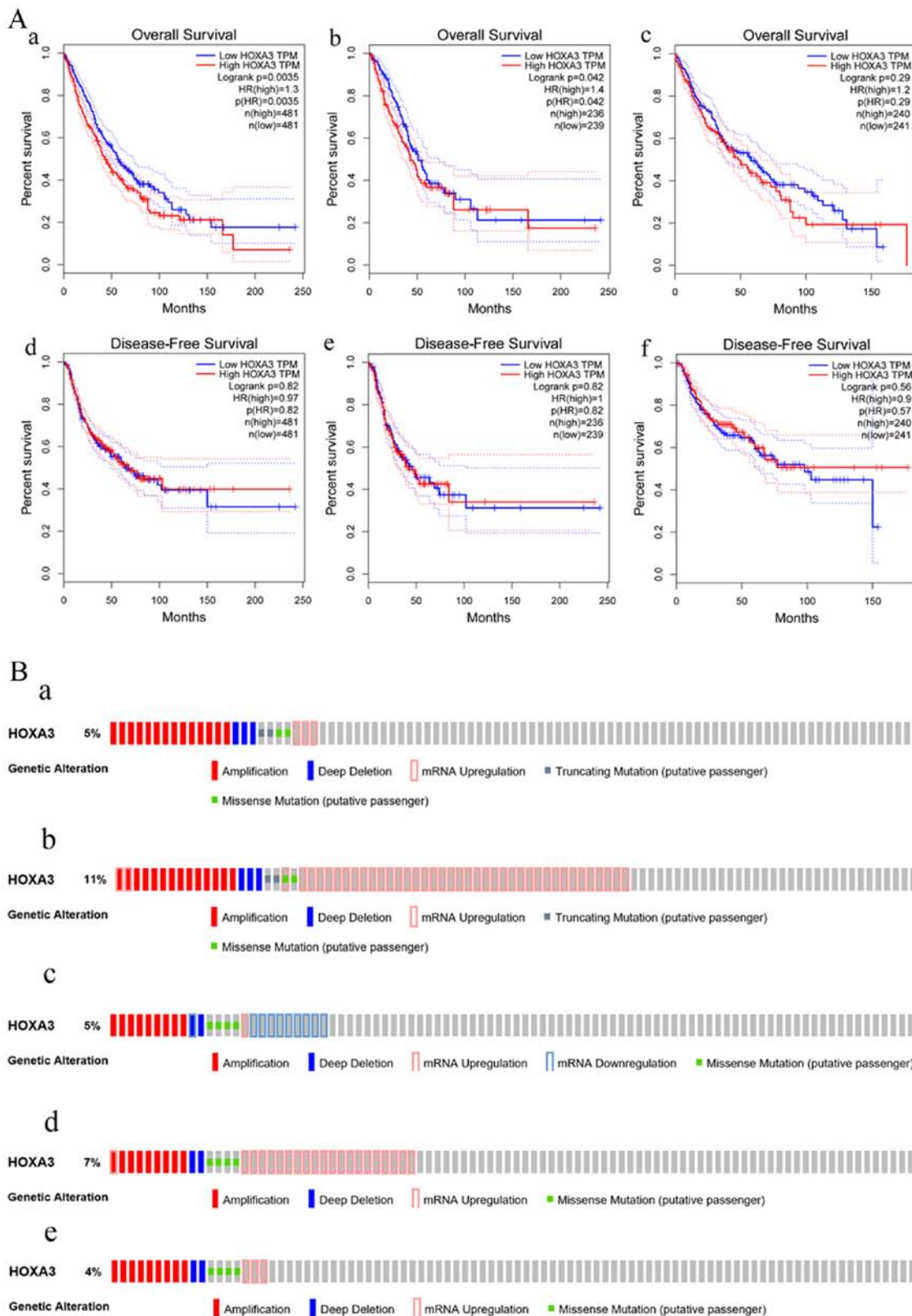
Figure 4. (A) Survival curve of HOXA3 expression in NSCLC. Overall survival (OS: panel a, NSCLC; panel b, LUAD; panel c, LUSC) and disease-free survival (DFS: panel d, NSCLC; panel e, LUAD; panel f, LUSC). (B) The atlas of genetic alteration of HOXA3 mRNA in NSCLC. Panels a and b show HOXA3 mRNA expression z-scores by microarray and RNA Seq V2 RSEM in LUAD. Altered were 24 (5%) and 59 (11%) of 520 sequenced cases/patients (520 total) respectively; panels c, d and e show HOXA3 mRNA expression z-scores by U133 microarray only, microarray and RNA Seq V2 RSEM in LUSC. Altered were 18 (4%), 25 (5%) and 35 (7%) of 504 sequenced cases/patients (504 total). HOXA3, homeobox A3; NSCLC, non-small cell lung cancer; LUAD, lung adenocarcinoma; LUSC, lung squamous cell carcinoma.

analysis revealed that genes in the NSCLC group mainly participated in biological processes, such as the regulation of

cell migration; the regulation of apoptosis; and the regulation of programmed cell death; cellular components, such as insoluble

Table II. The association of between the HOXA3 mRNA methylation level in NSCLC tissues and normal adjacent tissues base on the TCGA data.

		HOXA3 methylation level			t-test of data	
Histological type	Case no.	Mean	SD	FC	t-test	P-value
NSCLC						
Normal adjacent	86	0.43	0.11	1.00	9.89	<0.001
Cancer	744	0.57	0.21	1.32		
LUAD						
Normal adjacent	43	0.44	0.11	1.00	6.19	<0.001
Cancer	372	0.56	0.20	1.27		
LUSC						
Normal adjacent	43	0.42	0.11	1.00	7.72	<0.001
Cancer	372	0.58	0.21	1.38		

HOXA3, homeobox A3, an mRNA of homeobox genes of clusters A; NSCLC, non-small cell lung cancer; LUAD, lung adenocarcinoma; LUSC, lung squamous cell carcinoma.
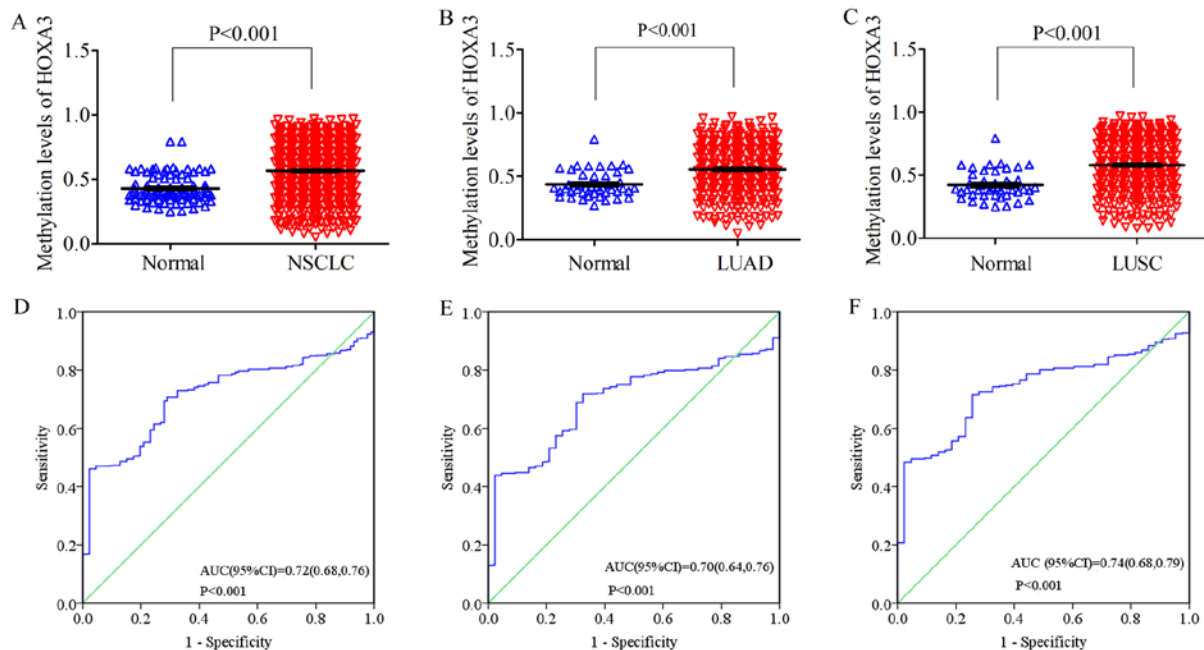

Figure 5. Scatter plot of HOXA3 methylation levels between lung cancer tissues and normal lung tissues (A) NSCLC; (B) LUAD; (C) LUSC. HOXA3, homeobox A3; NSCLC, non-small cell lung cancer; LUAD, lung adenocarcinoma; LUSC, lung squamous cell carcinoma; ROC curve of HOXA3 methylation levels between lung cancer tissues and normal lung tissues (D) NSCLC; (E) LUAD; (F) LUSC.

fraction, membrane fraction, and extracellular matrix; and molecular functions, such as sequence-specific DNA binding, enzyme activator activity, and phosphatidylinositol-3,4,5-tri-sphosphate binding (Figs. 6 and 8A-C, and Table III). The results of KEGG pathway analyses suggested that *HOXA3* may be involved in the functional regulation of 22 signalling pathways in the NSCLC group. The most important pathways were focal adhesion, pathways in cancer, and the TGF-β signalling pathway (Figs. 7 and 8D, and Table IV). In addition, genes in the LUAD group mainly participated in biological processes, such as the regulation of cell migration, regulation of apoptosis and the regulation of programmed cell death. Significant

enrichment also occurred in cellular components and molecular functions; for example, insoluble fraction and membrane fraction in cellular components and sequence-specific DNA binding and enzyme activator activity in molecular functions (Figs. 9 and 11A-C, and Table V). The analytical results in the LUAD group suggested that *HOXA3* may be involved in the biological regulation of 15 signalling pathways. Of these pathways, the most significant pathways were focal adhesion and ECM-receptor interaction (Figs. 10 and 11D, and Table VI). In PPI analyses, 278 interaction nodes were obtained in the NSCLC group (Fig. 12A). The genes with the top 10 overall scores are presented in Table VII. The results
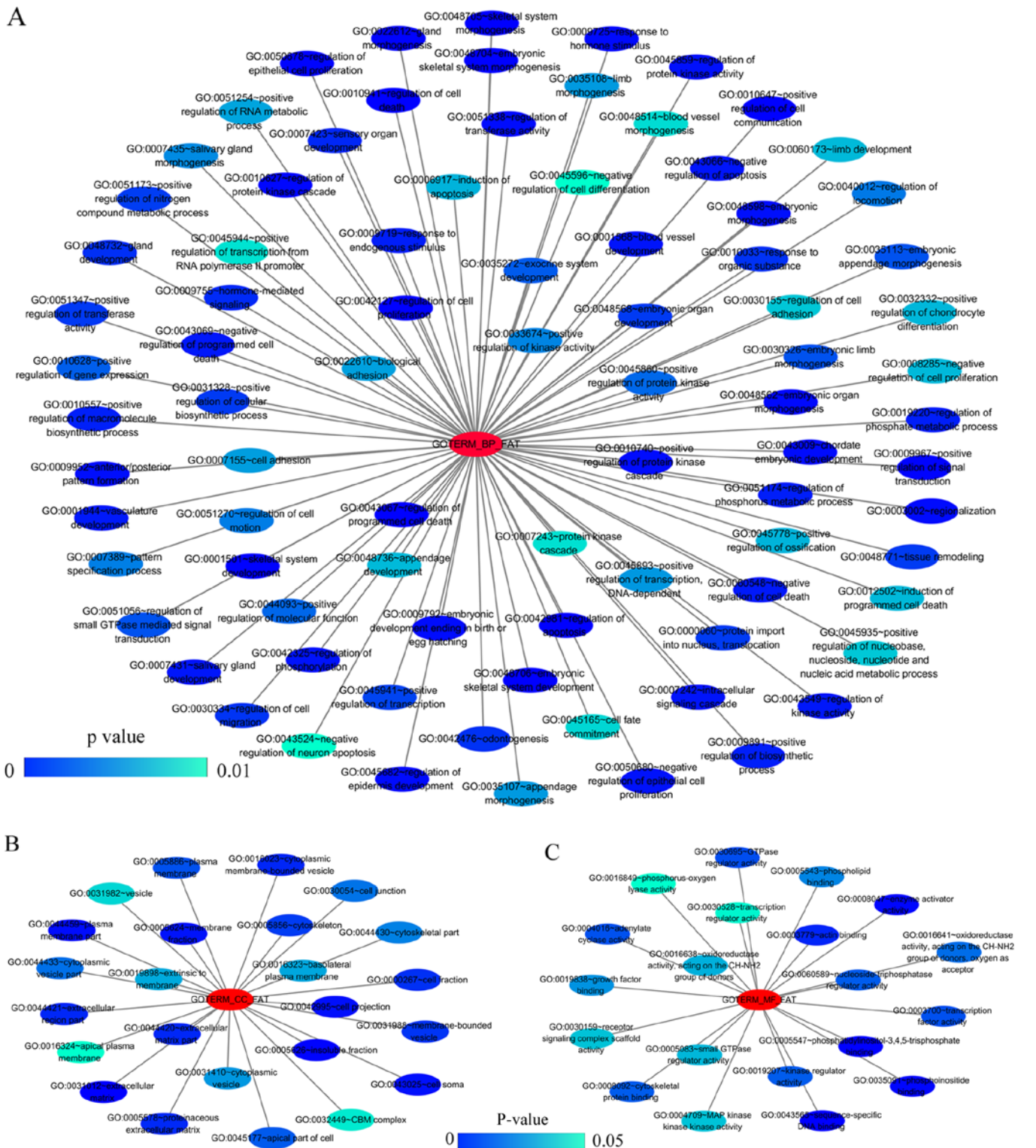
Figure 6. Network of gene ontology (GO) terms of HOXA3 co-expression genes in NSCLC constructed by cytoscape v3.5.0. (A-C) Show biological processes (BPs), cellular components (CCs) and molecular functions (MFs), respectively. In this network, only terms with statistically significant [P<0.01 (BP) or P<0.05 (CC and MF)] are displayed. Each node represents a GO term, and the node color indicates the P-value of a GO term. HOXA3, homeobox A3; NSCLC, non-small cell lung cancer.

of interaction network analyses demonstrated that *MAPK1*, *EGFR*, *DCN* and *CFTR* represented key genes in these networks. In addition, genes enriched in 'Focal adhesion' were used for PPI analyses, and a total of 13 interaction nodes were obtained (Fig. 12B). The genes with the top 10 overall score are presented in Table VIII. The results suggested that

MAPK1, *EGFR*, *TNC* and *COL1A1* were key genes in this pathway. PPI analyses were also performed on genes in the LUAD group, and the results generated 129 protein interaction nodes (Fig. 13). The nodes with the top 10 overall scores are presented in Table IX. The protein interaction network suggested that *MAPK1*, *EGFR*, *CFTR* and *GLI3* were key nodes
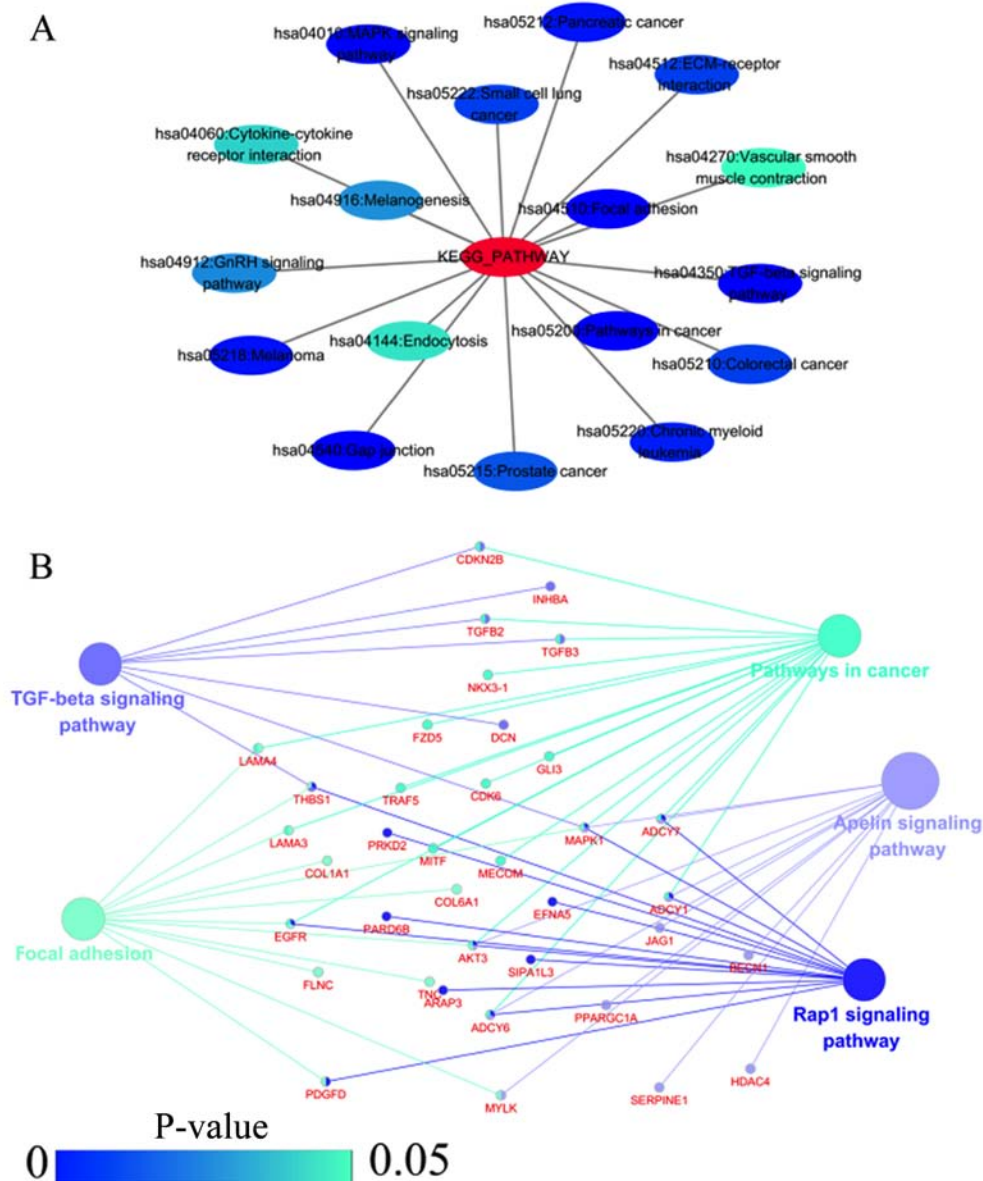
Figure 7. (A) Network mappings were Kyoto Encyclopedia of Genes and Genomes (KEGG) pathway of HOXA3 co-expression genes in NSCLC. (B) The significant signalling pathways (P<0.05) enriched in HOXA3 co-expression genes in NSCLC constructed by ClueGO plugin. The color of the circles represents the degree of enrichment of the pathway (P-value). HOXA3, homeobox A3; NSCLC, non-small cell lung cancer.

in these interaction networks. Genes in the LUAD group that were enriched in 'Focal adhesion' were used for PPI analyses, and 14 protein interaction network nodes were also obtained. The result was the same as that for the NSCLC group. *MAPK1*, *EGFR*, *TNC* and *COL1A1* were key genes in these pathways (refer to Fig. 12B and Table X). Analytic results revealed that genes in the NSCLC and LUAD groups all participated in the regulation of the 'Focal adhesion' pathway. *MAPK1* and *EGFR* played key roles in NSCLC and LUAD, whereas *MAPK1*, *EGFR*, *CFTR* and *GLI3* represented key genes in the 'Focal adhesion' pathway. Therefore, these 4 genes were analysed further. Based on TCGA data, the results of Pearson's correlation analysis revealed that the 4 genes, *EGFR*, *MAPK1*, *COL1A1* and *TNC*, all exhibited a potential positive correlation with *HOXA3* expression in NSCLC (Fig. 14). In the LUAD group, only *COL1A1* and *TNC* exhibited a possible positive correlation with *HOXA3* (Fig. 15C and D).

Prediction and preliminary validation of HOXA3 target miRNAs. *HOXA3* had 3 target miRNAs that passed the target prediction. Based on GEO microarray search and TCGA database, the random effects model was used for meta-analyses of the expression of these 3 miRNAs in NSCLC tissues. The results revealed that the expression of hsa-miR-372-3p was significantly increased in the NSCLC and LUAD tissues, but only exhibited an increasing trend in the LUSC tissues (NSCLC P<0.001, LUAD P=0.017, and LUSC P=0.243) (Fig. 16A). In addition, hsa-miR-372-3p and HOX3A had 1 fragment of complementary sequences of '3'CGUGAA5'-3' GCACUU-5'' (Fig. 16B). Furthermore, the sensitivity and specificity of miR-372-3p expression in NSCLC were examined using the sROC method. The results suggested that the optimal sensitivity and specificity of a high miR-372-3p expression in the NSCLC group were SENS, 0.71 (0.57, 0.83) and SPES, 0.65 (0.52, 0.76), respectively, and

Table III. The top ten most significant items of Gene Ontology (GO) terms of the co-expression genes of homeobox A3 (HOXA3) in non-small cell lung cancer.

Category	Term	Count	P-value	FDR
Biological processes				
GOTERM_BP_FAT	GO:0048706~embryonic skeletal system development	8	3.41E-05	0.06
GOTERM_BP_FAT	GO:0001501~skeletal system development	14	1.07E-04	0.18
GOTERM_BP_FAT	GO:0045682~regulation of epidermis development	5	1.17E-04	0.19
GOTERM_BP_FAT	GO:0030334~regulation of cell migration	10	1.80E-04	0.30
GOTERM_BP_FAT	GO:0042981~regulation of apoptosis	23	1.97E-04	0.33
GOTERM_BP_FAT	GO:0043067~regulation of programmed cell death	23	2.27E-04	0.38
GOTERM_BP_FAT	GO:0010941~regulation of cell death	23	2.39E-04	0.40
GOTERM_BP_FAT	GO:0048705~skeletal system morphogenesis	8	3.64E-04	0.60
GOTERM_BP_FAT	GO:0040012~regulation of locomotion	10	4.64E-04	0.77
GOTERM_BP_FAT	GO:0051270~regulation of cell motion	10	4.81E-04	0.80
Cellular components				
GOTERM_CC_FAT	GO:0005626~insoluble fraction	22	0.000184	0.24
GOTERM_CC_FAT	GO:0005624~membrane fraction	20	0.000837	1.07
GOTERM_CC_FAT	GO:0031012~extracellular matrix	12	0.001071	1.37
GOTERM_CC_FAT	GO:0044420~extracellular matrix part	7	0.001490	1.90
GOTERM_CC_FAT	GO:0045177~apical part of cell	8	0.002892	3.66
GOTERM_CC_FAT	GO:0000267~cell fraction	22	0.004675	5.86
GOTERM_CC_FAT	GO:0042995~cell projection	16	0.006747	8.35
GOTERM_CC_FAT	GO:0005578~proteinaceous extracellular matrix	10	0.006859	8.48
GOTERM_CC_FAT	GO:0016324~apical plasma membrane	6	0.013372	15.92
GOTERM_CC_FAT	GO:0016323~basolateral plasma membrane	7	0.020688	23.61
Molecular functional				
GOTERM_MF_FAT	GO:0043565~sequence-specific DNA binding	20	0.000041	0.06
GOTERM_MF_FAT	GO:0008047~enzyme activator activity	11	0.004149	5.55
GOTERM_MF_FAT	GO:0005547~phosphatidylinositol-3,4,5-trisphosphate binding	3	0.004179	5.59
GOTERM_MF_FAT	GO:0016641~oxidoreductase activity, acting on the CH-NH2 group of donors, oxygen as acceptor	3	0.010187	13.11
GOTERM_MF_FAT	GO:0030695~GTPase regulator activity	11	0.014540	18.21
GOTERM_MF_FAT	GO:0016638~oxidoreductase activity, acting on the CH-NH2 group of donors	3	0.016640	20.58
GOTERM_MF_FAT	GO:0060589~nucleoside-triphosphatase regulator activity	11	0.016712	20.66
GOTERM_MF_FAT	GO:0035091~phosphoinositide binding	5	0.025094	29.45
GOTERM_MF_FAT	GO:0016208~AMP binding	3	0.028747	33.00
GOTERM_MF_FAT	GO:0003779~actin binding	9	0.028844	33.09

the AUC was 0.73 (95% CI: 0.69, 0.77). The optimal sensitivity and specificity of the LUAD group were SENS, 0.65 (0.5, 0.77) and SPES, 0.66 (0.43, 0.83), respectively, and the AUC was 0.69 (95% CI: 0.65, 0.73) (Fig. 16C and D).

Discussion

This study used qPCR detection and TCGA RNA-seq data to confirm that *HOXA3* expression was significantly down-regulated in LUAD tissues. The downregulation of *HOXA3* may be closely associated with a more favourable prognosis of LUAD. In addition, the TCGA data indicated that *HOXA3* harboured genetic alterations in 11-55% of LUAD tissues, and the methylation level of *HOXA3* in LUAD tissues was significantly upregulated. Combined with the TCGA data, the upregulation of the *HOXA3* level in LUSC was not significant. Therefore, we paid more attention to the clinical significance and molecular mechanisms of action of *HOXA3* in LUAD. Through the collection of co-expression genes and GO and KEGG analyses, the preliminary results revealed that *HOXA3* may play important roles in LUAD through the regulation of focal adhesion and ECM-receptor interaction signalling pathways. Furthermore, through the prediction of *HOXA3* target miRNAs and meta-analyses of target miRNA expression based on the GEO microarray and TCGA data, the results confirmed that the expression of miR-372-3p that had complementary sequences with *HOXA3* was significantly increased in LUAD tissues.

Table IV. KEGG pathways enriched by co-expression genes of homeobox A3 (HOXA3) mRNA in non-small cell lung cancer.

| Category	Term	Count	P-value	FDR
KEGG_PATHWAY	hsa04510:Focal adhesion	12	0.001	0.76
KEGG_PATHWAY	hsa05200:Pathways in cancer	15	0.001	1.67
KEGG_PATHWAY	hsa04350:TGF-beta signaling pathway	7	0.004	4.34
KEGG_PATHWAY	hsa04540:Gap junction	7	0.004	4.84
KEGG_PATHWAY	hsa04010:MAPK signaling pathway	12	0.006	7.01
KEGG_PATHWAY	hsa05218:Melanoma	6	0.008	8.33
KEGG_PATHWAY	hsa05212:Pancreatic cancer	6	0.008	8.81
KEGG_PATHWAY	hsa05220:Chronic myeloid leukemia	6	0.010	10.36
KEGG_PATHWAY	hsa05222:Small cell lung cancer	6	0.015	15.93
KEGG_PATHWAY	hsa05210:Colorectal cancer	6	0.015	15.93
KEGG_PATHWAY	hsa04512:ECM-receptor interaction	6	0.015	15.93
KEGG_PATHWAY	hsa05215:Prostate cancer	6	0.019	19.63
KEGG_PATHWAY	hsa04912:GnRH signaling pathway	6	0.028	27.23
KEGG_PATHWAY	hsa04916:Melanogenesis	6	0.029	28.15
KEGG_PATHWAY	hsa04060:Cytokine-cytokine receptor interaction	10	0.039	35.71
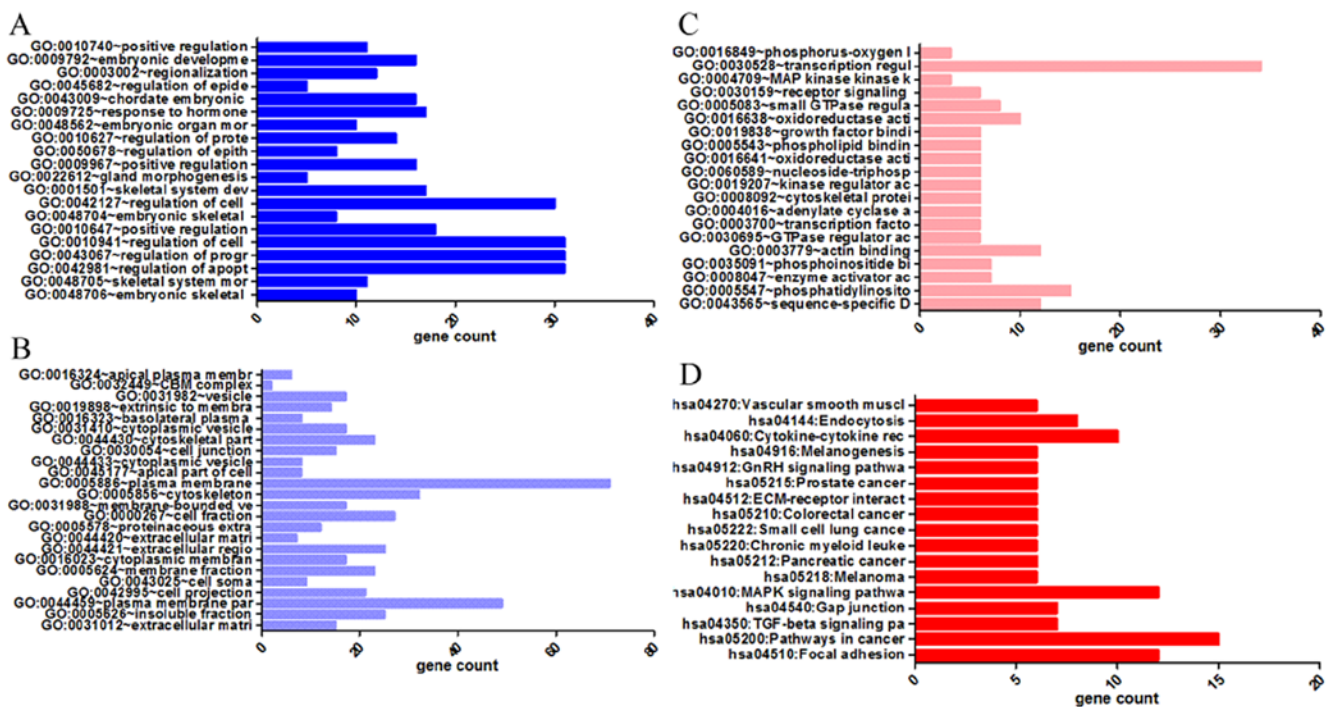
Figure 8. Significantly enriched annotation of GO categories and KEGG pathways of HOXA3 co-expression genes in NSCLC. (A) Biological processes (BPs); (B) Cellular components (CCs); (C) Molecular factors (MFs); (D) KEGG pathways. GO, Gene Ontology; KEGG, Kyoto Encyclopedia of Genes and Genomes; HOXA3, homeobox A3; NSCLC, non-small cell lung cancer.

There have been some studies of the association between the *HOXA3* level and tumours. For example, Zhang *et al* (30) demonstrated that *HOXA3* exhibited a high expression in both colorectal cancer tissues and cell lines. Shen *et al* (31) assessed the association between HOX family genes and nasopharyngeal carcinoma and demonstrated that *HOXA3* expression was also upregulated. Kuasne *et al* (32) suggested that *HOXA3* exhibited a low expression in penile carcinoma. At least to the best of our knowledge, only 1 methylation-related study on the association between *HOXA3* and LUAD

has been reported (19). This study, to the best of our knowledge, was the first to detect *HOXA3* mRNA expression in LUAD. Combined with qPCR detection and TCGA data, we confirmed that *HOXA3* expression was downregulated in LUAD tissues, and a low *HOXA3* expression may play a important role in LUAD.

The investigation of the association between *HOXA3* and tumour progression has demonstrated that a high *HOXA3* expression is associated with low survival rates in colon cancer (33). In penile carcinoma, a low *HOXA3* expression was

Table V. The top 10 most significant items of Gene Ontology (GO) terms of the co-expression genes of homeobox A3 (HOXA3) mRNA in lung adenocarcinoma.

Category	Term	Count	P-value	FDR
Biological Processes				
GOTERM_BP_FAT	GO:0048706~embryonic skeletal system development	8	3.41E-05	0.056837
GOTERM_BP_FAT	GO:0001501~skeletal system development	14	1.07E-04	0.178201
GOTERM_BP_FAT	GO:0045682~regulation of epidermis development	5	1.17E-04	0.194494
GOTERM_BP_FAT	GO:0030334~regulation of cell migration	10	1.80E-04	0.299680
GOTERM_BP_FAT	GO:0042981~regulation of apoptosis	23	1.97E-04	0.328453
GOTERM_BP_FAT	GO:0043067~regulation of programmed cell death	23	2.27E-04	0.377505
GOTERM_BP_FAT	GO:0010941~regulation of cell death	23	2.39E-04	0.397502
GOTERM_BP_FAT	GO:0048705~skeletal system morphogenesis	8	3.64E-04	0.604848
GOTERM_BP_FAT	GO:0040012~regulation of locomotion	10	4.64E-04	0.770756
GOTERM_BP_FAT	GO:0051270~regulation of cell motion	10	4.81E-04	0.798787
Cellular ψomponents				
GOTERM_CC_FAT	GO:0005626~insoluble fraction	22	0.000184	0.237025
GOTERM_CC_FAT	GO:0005624~membrane fraction	20	0.000837	1.072817
GOTERM_CC_FAT	GO:0031012~extracellular matrix	12	0.001071	1.370868
GOTERM_CC_FAT	GO:0044420~extracellular matrix part	7	0.001490	1.902184
GOTERM_CC_FAT	GO:0045177~apical part of cell	8	0.002892	3.662636
GOTERM_CC_FAT	GO:0000267~cell fraction	22	0.004675	5.857488
GOTERM_CC_FAT	GO:0042995~cell projection	16	0.006747	8.351548
GOTERM_CC_FAT	GO:0005578~proteinaceous extracellular matrix	10	0.006859	8.483923
GOTERM_CC_FAT	GO:0016324~apical plasma membrane	6	0.013372	15.921503
GOTERM_CC_FAT	GO:0016323~basolateral plasma membrane	7	0.020688	23.607821
Molecular φunctional				
GOTERM_MF_FAT	GO:0043565~sequence-specific DNA binding	20	0.000041	0.056109
GOTERM_MF_FAT	GO:0008047~enzyme activator activity	11	0.004149	5.548392
GOTERM_MF_FAT	GO:0005547~phosphatidylinositol-3,4,5-trisphosphate binding	3	0.004179	5.587211
GOTERM_MF_FAT	GO:0016641~oxidoreductase activity, acting on the CH-NH2 group of donors, oxygen as acceptor	3	0.010187	13.113973
GOTERM_MF_FAT	GO:0030695~GTPase regulator activity	11	0.014540	18.214548
GOTERM_MF_FAT	GO:0016638~oxidoreductase activity, acting on the CH-NH2 group of donors	3	0.016640	20.575093
GOTERM_MF_FAT	GO:0060589~nucleoside-triphosphatase regulator activity	11	0.016712	20.655661
GOTERM_MF_FAT	GO:0035091~phosphoinositide binding	5	0.025094	29.453780
GOTERM_MF_FAT	GO:0016208~AMP binding	3	0.028747	32.997529
GOTERM_MF_FAT	GO:0003779~actin binding	9	0.028844	33.089357

found to be associated with a poor prognosis (32). However, the association between *HOXA3* and the progression of nasopharyngeal carcinoma has not been studied in depth (31). Our analyses of *HOXA3* expression in all pathological stages of LUAD did not exhibit an obvious pattern. The survival analyses demonstrated that patients LUAD with a low *HOXA3* expression had a better OS. Therefore, we hypothesized that the downregulation of *HOXA3* expression may be an independent protective factor in LUAD.

Furthermore, based on the microarray and RNA Seq data in TCGA, we preliminarily revealed that *HOXA3* harboured a certain level of genetic alterations in LUAD tumour tissues. Thus, we would like to acquire more information for further validation. However, relevant studies are currently lacking,

and literature reports are not available, at least to the best of our knowledge. As regards gene methylation, Kuasne *et al* performed genome-wide methylation studies on penile carcinoma and confirmed that 8 genes, including *HOXA3*, exhibited high methylation levels (32). In a validation study of epigenetic biomarkers in LUAD, Daugaard *et al* (19) performed genome-wide methylation microarray sequencing on 4 cases of LUAD tissues and normal cancer-adjacent lung tissues to screen differentially methylated genes in LUAD. They selected the 18 most significantly differentially methylated genes, including *HOXA3*, for validation in 52 samples. The methylation level of *HOXA3* significantly increased (19). This study acquired *HOXA3* methylation data from the TCGA database to perform analyses. The results suggested that the *HOXA3* methylation
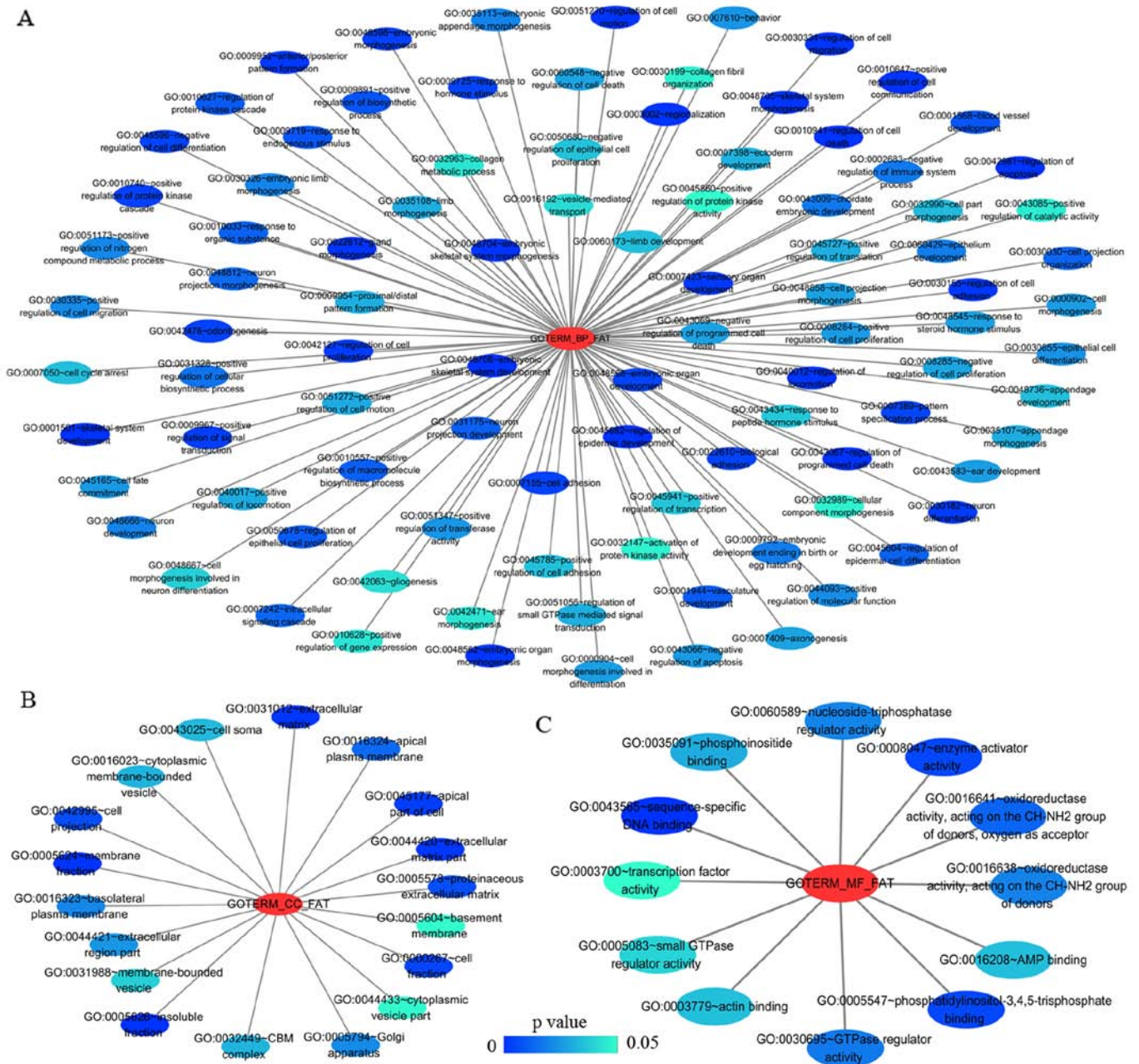
Figure 9. The network of GO terms of HOXA3 co-expression genes in LUAD were constructed by cytoscape v3.5.0. (A-C) Biological processes (BPs), cellular components (CCs) and molecular functions (MFs), respectively. In this network, only terms with statistically significant (P<0.05) are displayed. Each node represents a GO term, and the node color indicates the P-value of a GO term. GO, Gene Ontology; HOXA3, homeobox A3; LUAD, lung adenocarcinoma.

level was significantly increased in LUAD tissues. This finding was consistent with the results in literature reports. Combined with *HOXA3* mRNA expression levels in LUAD, the function of *HOXA3* in LUAD may be associated with the increase in the methylation level. In addition, the study by Daugaard also demonstrated that the increase of *HOXA3* methylation was even more evident in patients with tumour metastasis; however, its association with the prognostic survival rates in LUAD patients has not been elucidated (19). Despite the results of this study, sufficient evidence is not yet available to confirm the association between the methylation level of *HOXA3* and LUAD progression. Thus, further studies are required for confirmation. As regards studies on the association between DNA methylation and mRNA expression, Kuasne *et al* (32)

performed qPCR detection to demonstrate that genes with high methylation levels exhibited a low expression in penile carcinoma. These results confirmed that the methylation level and mRNA expression exhibited a negative correlation (32). Zhang *et al* performed cell experiments to confirm that a group of genes (*S100P*, *GDA*, *WISP2*, *LOXL1*, *TIMP4*, *ICAM1*, *CLMP*, *HSP8*, *GAS1* and *BMP2*) exhibited a downregulated mRNA expression through high methylation levels to induce drug resistance in NSCLC (34). Jin *et al* demonstrated that 19 genes mediated the downregulation of mRNA expression through the increase in upstream methylation levels in LUAD (35). This study confirmed the low expression of *HOXA3* in LUAD and the increase in the methylation level. Based on these findings, we hypothesized that *HOXA3*

Table VI. KEGG pathway enriched by co-expression genes of homeobox A3 (HOXA3) mRNA in lung adenocarcinoma.

Category	Term	Count	P-value	FDR
KEGG_PATHWAY	hsa04510:Focal adhesion	12	3.84E-05	0.042706
KEGG_PATHWAY	hsa04512:ECM-receptor interaction	6	0.004145	4.514261
KEGG_PATHWAY	hsa05218:Melanoma	5	0.012451	13.009202
KEGG_PATHWAY	hsa05212:Pancreatic cancer	5	0.013063	13.603250
KEGG_PATHWAY	hsa05210:Colorectal cancer	5	0.021874	21.802852
KEGG_PATHWAY	hsa05222:Small cell lung cancer	5	0.021874	21.802852
KEGG_PATHWAY	hsa05200:Pathways in cancer	10	0.022490	22.349251
KEGG_PATHWAY	hsa05215:Prostate cancer	5	0.026406	25.738703
KEGG_PATHWAY	hsa05223:Non-small cell lung cancer	4	0.031134	29.652037
KEGG_PATHWAY	hsa05214:Glioma	4	0.045993	40.760927
KEGG_PATHWAY	hsa04010:MAPK signaling pathway	8	0.052597	45.164053
KEGG_PATHWAY	hsa05220:Chronic myeloid leukemia	4	0.070302	55.541161
KEGG_PATHWAY	hsa04144:Endocytosis	6	0.084942	62.734617
KEGG_PATHWAY	hsa04350:TGF-beta signaling pathway	4	0.099275	68.735075
KEGG_PATHWAY	hsa04012:ErbB signaling pathway	4	0.099275	68.735075

Table VII. Top 10 with combined co-expression score that the protein-protein interaction (PPI) of homeobox A3 (HOXA3) co-expression genes in non-small cell lung cancer.

#Node1	Node2	Node1 STRING internal ID	Homology	Co-expression	Experimentally determined interaction	Automated text mining	Combined score
STX2	SNAP25	1858001	0	0.093	0.939	0.905	0.998
CDKN2B	CDK6	1846519	0	0.054	0.432	0.763	0.985
DUSP10	MAPK1	1854467	0	0.053	0.498	0.705	0.984
CALD1	MYLK	1854225	0	0.248	0	0.791	0.982
MITF	MAPK1	1847592	0	0.048	0.395	0.733	0.982
ARRB1	MAPK1	1860799	0	0	0.43	0.658	0.978
ITSN1	ITSN2	1857363	0.965	0	0.702	0.726	0.969
EGFR	MAPK1	1846445	0.632	0	0.503	0.932	0.965
MALT1	CARD10	1850132	0	0	0.115	0.63	0.964
RUNX2	MAPK1	1855482	0	0	0	0.639	0.962

methylation has a negative regulatory association with mRNA expression and plays critical roles in tumour development and progression.

To investigate the underlying molecular mechanisms, GO and KEGG analyses were performed to compare the enrichment of *HOXA3* co-expression genes between the NSCLC group and the LUAD group. The results demonstrated that the enrichment conditions in biological processes, cellular components, and molecular functions were basically the same. Some differences in the KEGG signalling pathways were noted. The LUAD group was more concentrated on the focal adhesion and ECM-receptor interaction pathways. *HOXA3* may carry out its regulatory functions in LUAD through participation in these 2 signalling pathways. The focal adhesion signalling pathway is a critical pathway to activate focal adhesion kinase (FAK). Kinases activated by this pathway mainly mediate a variety of cellular metabolic processes, including cell metastasis, growth

factor signal transduction, cell survival, cell cycle progression, and cell movement, and are closely associated with the development of malignant tumours (36-38). Currently, there are literature reports on using FAK as a novel potential biological target to investigate targeted therapy of NSCLC (39,40). The ECM-receptor interaction signalling pathway mediates the expression of enriched genes and regulates functions of these genes to promote tumour cell proliferation and migration and participate in tumour metastasis and infiltration (41,42). In NSCLC unrelated to smoking, the ECM-receptor interaction signalling pathway plays a critical role (43). The above-mentioned 2 signalling pathways significantly influence the development and progression of human malignant tumours and act as the bridge between abnormal gene expression and malignant tumour development.

Therefore, in this study, we performed PPI analyses on genes enriched in the focal adhesion and ECM-receptor interaction
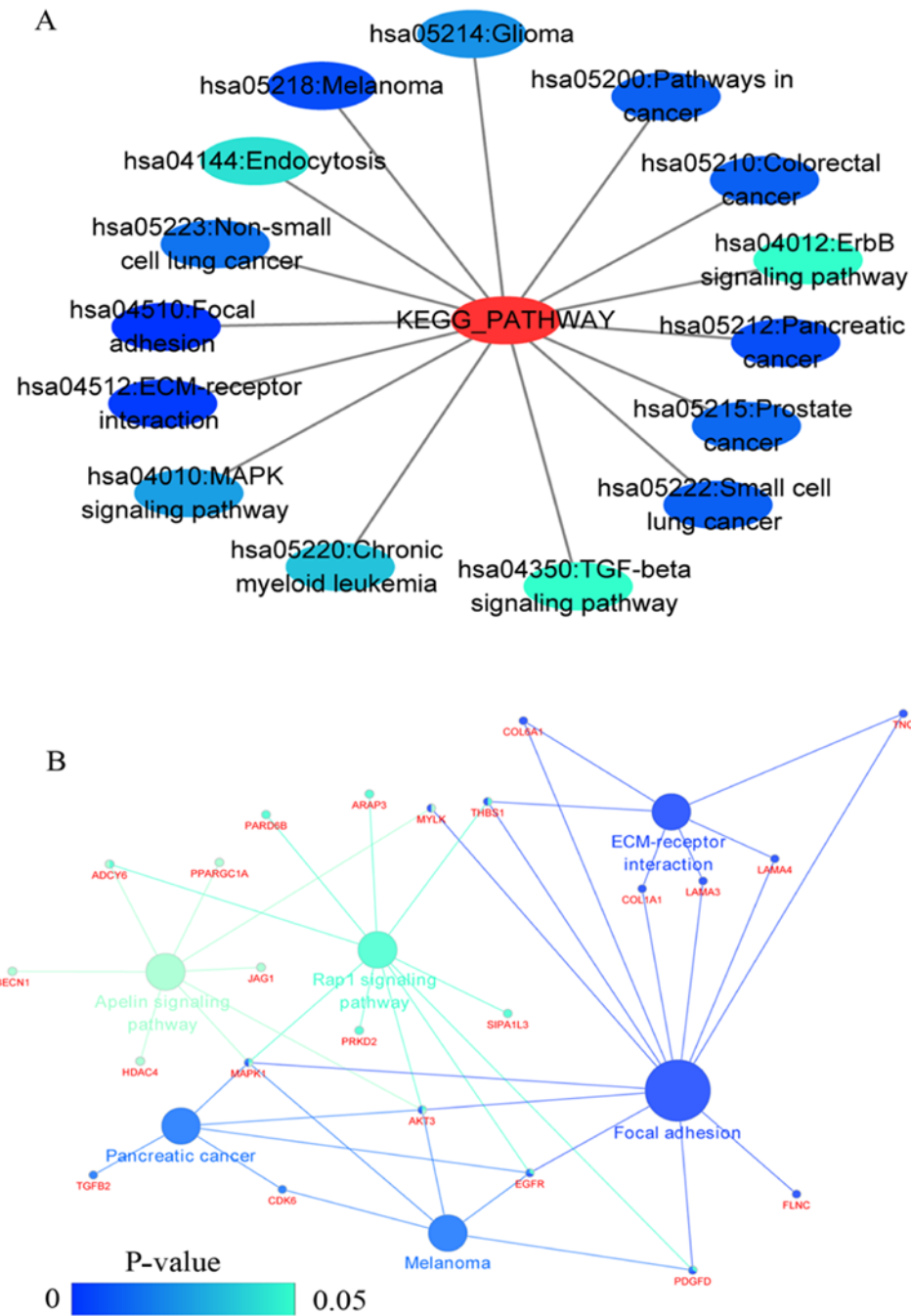
Figure 10. (A) Network mappings of KEGG pathway anlaysis of HOXA3 co-expression genes in LUAD. (B) The significantly signalling pathways (P<0.05) enriched HOXA3 co-expression genes in LUAD constructed by the ClueGO plugin. The color of circles represents the P-value of the signalling pathways. HOXA3, homeobox A3; KEGG, Kyoto Encyclopedia of Genes and Genomes; LUAD, lung adenocarcinoma.

signalling pathways and demonstrated that *MAPK1*, *EGFR*, *TNC* and *COL1A1* served as core genes in these 2 pathways. In addition, based on the TCGA data, Pearson's correlation analyses demonstrated that only *TNC* and *COL1A1* exhibited significantly positive correlations with *HOXA3* expression in LUAD. One relevant study detected 72 cases of NSCLC tissues and normal lung tissues (44). *TNC* expression was upregulated in NSCLC and dwas closely associated with TNM stage, lymph node metastasis and tumour pleural invasion. Other studies have also demonstrated that *TNC* upregulation is associated with a poor prognosis in LUAD (45,46). The study by Oleksiewicz *et al* (47) on 156 cases of NSCLC and

normal lung tissues revealed that *COL1A1* was significantly overexpressed in tumour tissues. That study also performed cell experiments to confirm that *COL1A1* was closely associated with hypoxia responses in NSCLC (47). Combined with bioinformatics analysis results, *HOXA3* may collaborate with co-expression genes, such as *TNC* and *COL1A1*, to regulate focal adhesion and ECM-receptor interaction signalling pathways, thus carrying out is functions in LUAD. However, more functional studies are required for further validation.

In this study, we also performed meta-analyses to confirm that the expression of the predicted miR-372-3p was upregulated in LUAD. Complementary sequences were noted

Table VIII. Top 10 with combined co-expression score that the protein-protein interaction (PPI) of homeobox A3 (HOXA3) co-expression gene intersection in non-small cell lung cancer enriched in significant signalling pathways.

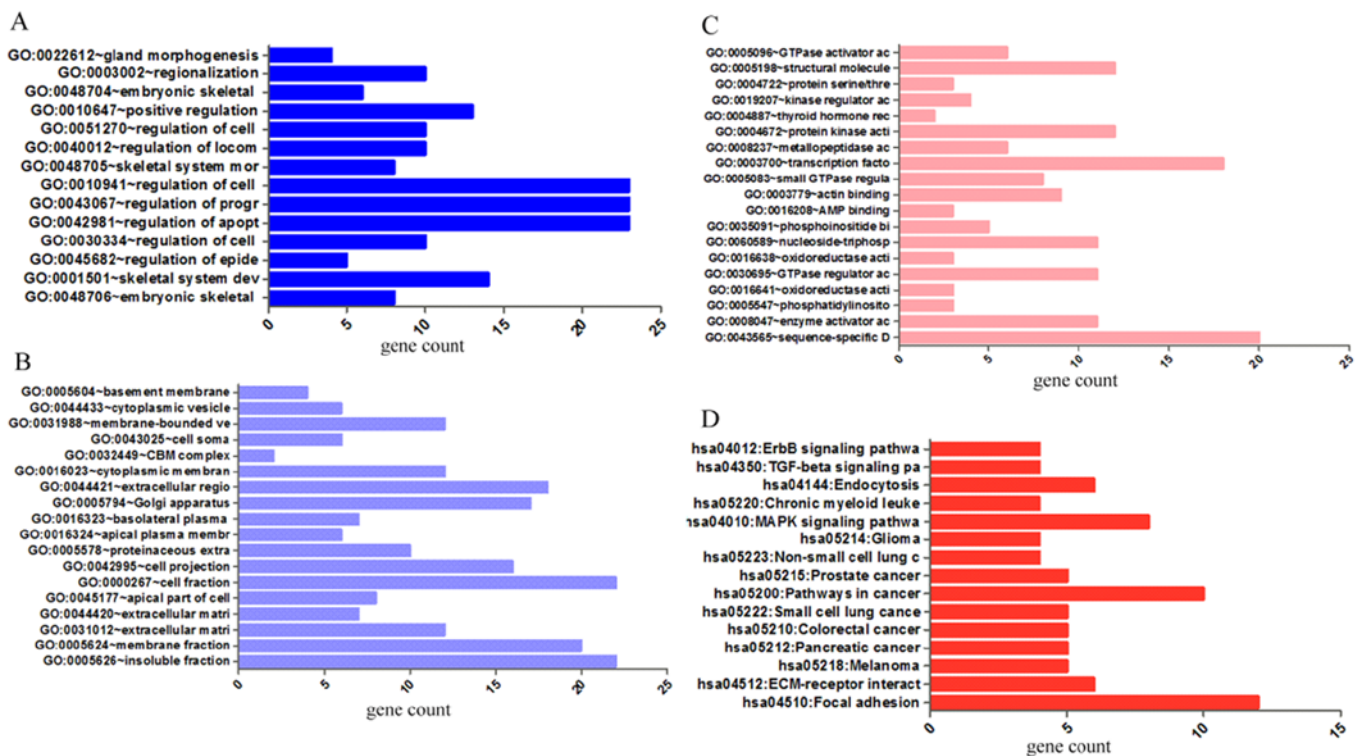| #Node1	Node2	Node1 STRING internal ID	Homology	Co-expression	Experimentally determined interaction	Automated text mining	Combined score
EGFR	MAPK1	1846445	0.632	0	0.503	0.932	0.965
COL6A1	COL1A1	1854318	0.617	0.504	0	0.49	0.957
MYLK	MAPK1	1853981	0.636	0	0	0.711	0.925
LAMA3	LAMA4	1850649	0.804	0	0	0.115	0.901
PDGFD	EGFR	1858075	0	0	0	0.49	0.893
EGFR	TNC	1846445	0	0	0.36	0.72	0.813
THBS1	COL1A1	1844779	0	0.1	0.324	0.463	0.645
TNC	MAPK1	1845696	0	0	0	0.576	0.576
TNC	THBS1	1845696	0	0.052	0	0.533	0.538
FLNC	MAPK1	1850897	0	0	0.066	0.475	0.49
EGFR	MAPK1	1846445	0.632	0	0.503	0.932	0.965
COL6A1	COL1A1	1854318	0.617	0.504	0	0.49	0.957
MYLK	MAPK1	1853981	0.636	0	0	0.711	0.925
LAMA3	LAMA4	1850649	0.804	0	0	0.115	0.901
PDGFD	EGFR	1858075	0	0	0	0.49	0.893

Figure 11. Significantly enriched annotation of GO categories and KEGG pathways of HOXA3 co-expression genes in LUAD. (A) Biological processes (BPs); (B) Cellular components (CCs); (C) Molecular factors (MFs); (D) KEGG pathway. HOXA3, homeobox A3; GO, Gene Ontology; KEGG, Kyoto Encyclopedia of Genes and Genomes; LUAD, lung adenocarcinoma.

between miR-372-3p and *HOXA3*. Combined with qPCR detection, *HOXA3* and miR-372-3p expression exhibited a negative correlation trend in LUAD. The results of a literature search demonstrated that miR-372-3p was highly expressed in both testicular cancer and LUSC. miR-372-3p promotes cell growth and migration in LUSC through the downregulation of the target gene *FGF9* (48,49). Therefore, based on results of this study and those of studies in the literature, we hypothesized that the downregulation of *HOXA3* expression in LUAD tissues may be associated with the increase in miR-372-3p
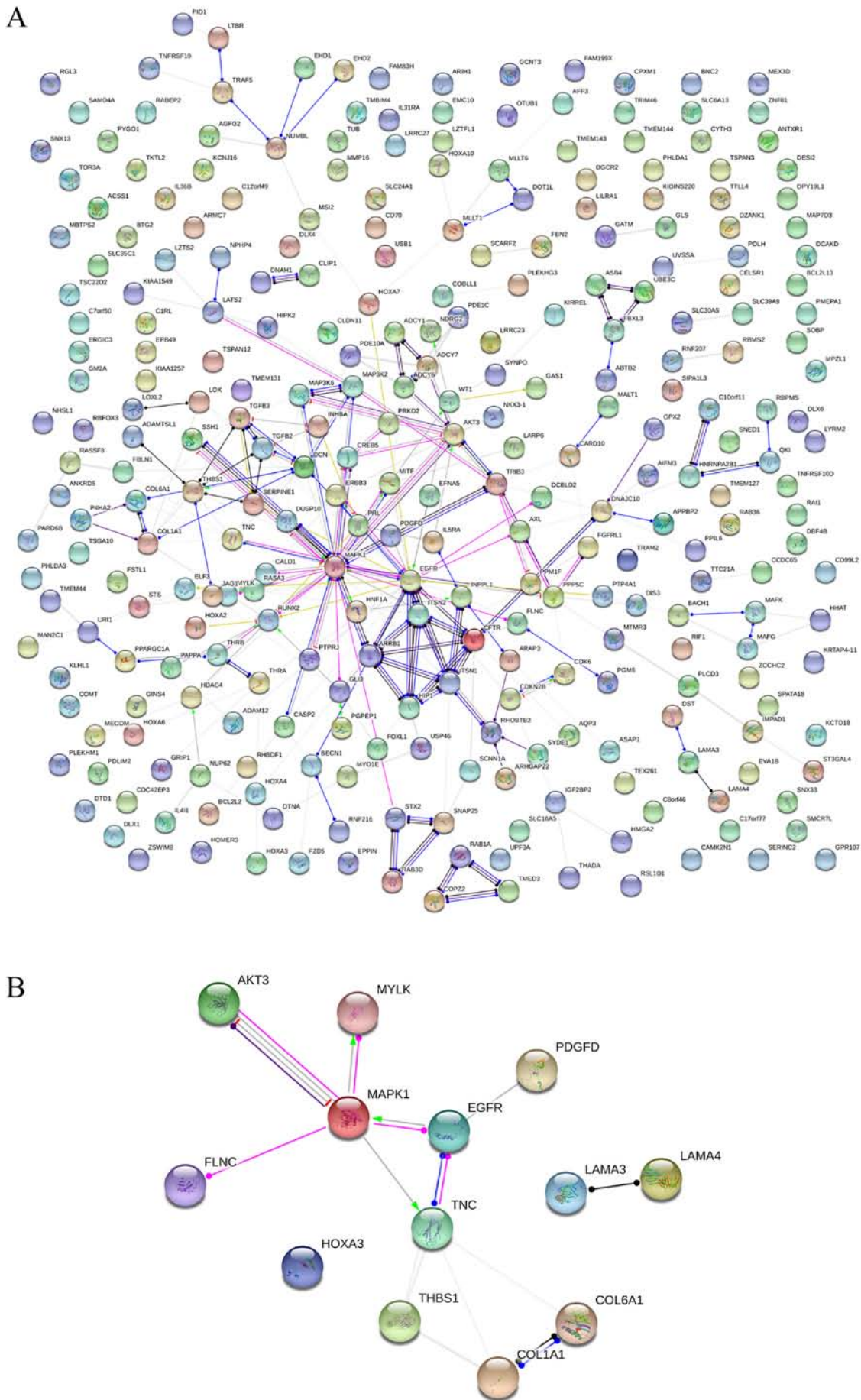
Figure 12. (A) PPI network analysis of genes co-expressed in HOXA3 in NSCLC and (B) the genes most implicated by the signalling pathways. PPI, protein-protein interaction; HOXA3, homeobox A3; NSCLC, non-small cell lung cancer.
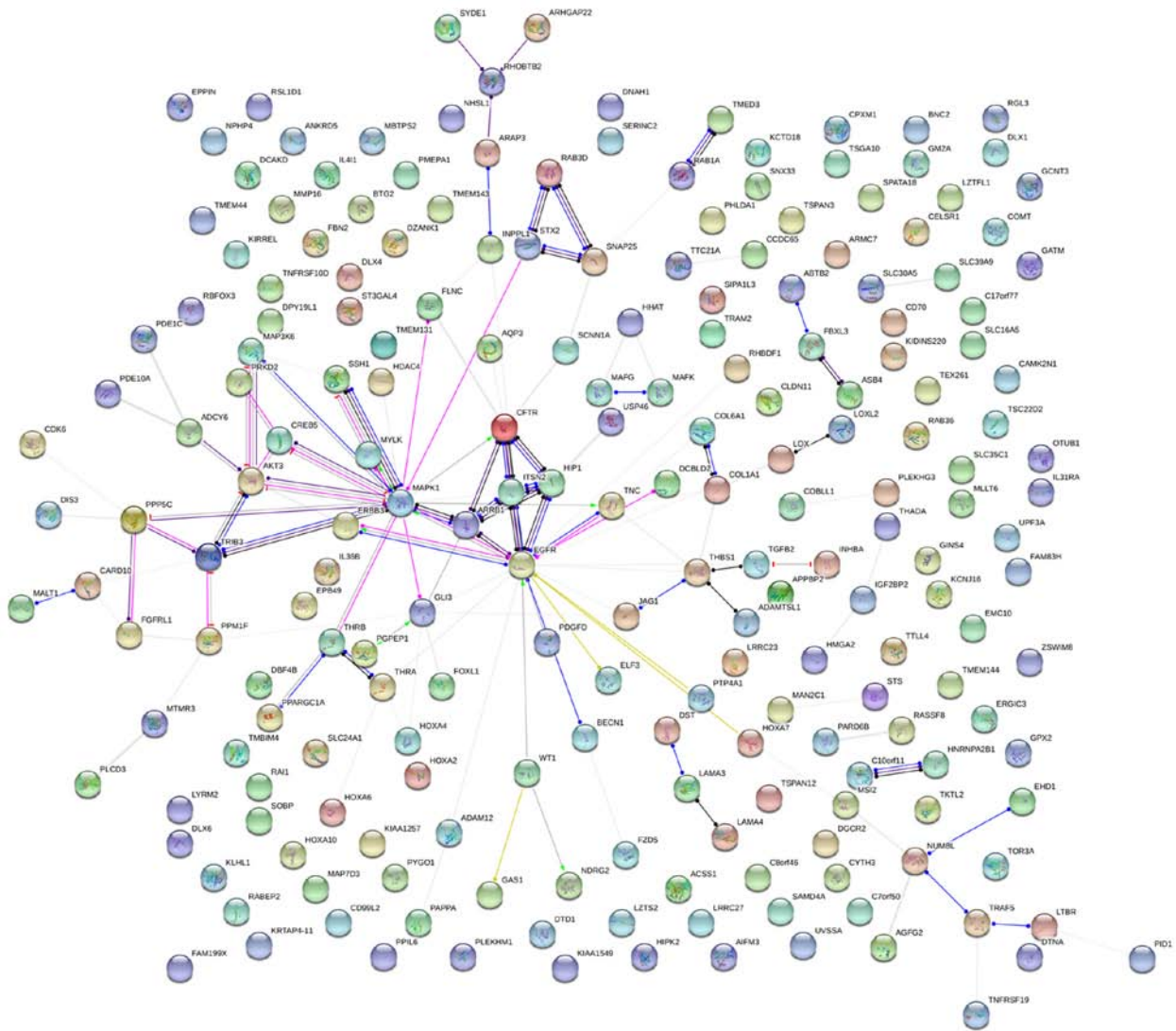
Figure 13. PPI network analysis of genes co-expressed in HOXA3 in LUAD. PPI, protein-protein interaction; HOXA3, homeobox A3; LUAD, lung adenocarcinoma.
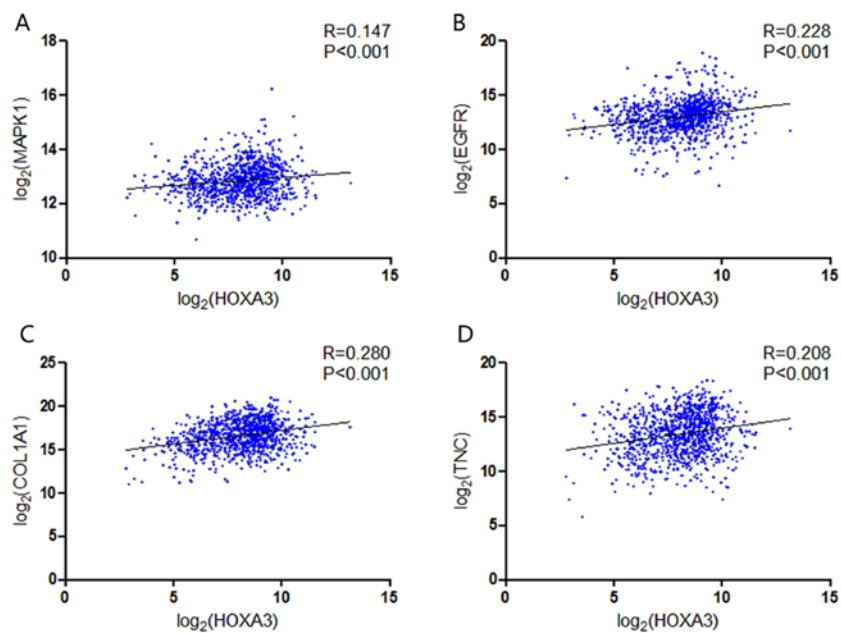

Figure 14. Correlation between the hub genes and the expression of HOXA3 in NSCLC. (A) MAPK1; (B) EGFR; (C) COL1A1; (D) TNC. HOXA3, homeobox A3; NSCLC, non-small cell lung cancer.
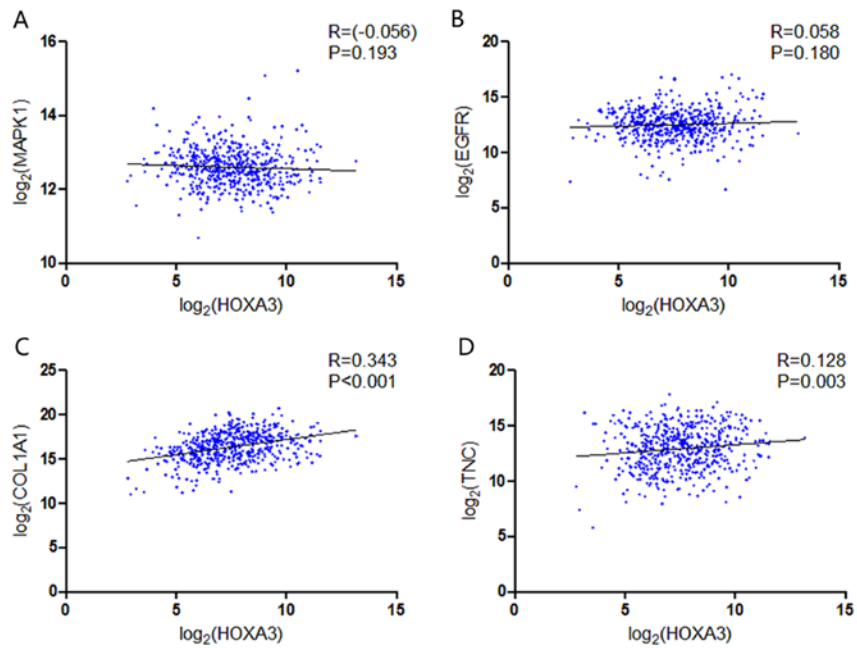
Figure 15. Correlation between the hub genes and the expression of HOXA3 in LUAD. (A) MAPK1; (B) EGFR; (C) COL1A1; (D) TNC. HOXA3, homeobox A3; LUAD, lung adenocarcinoma.
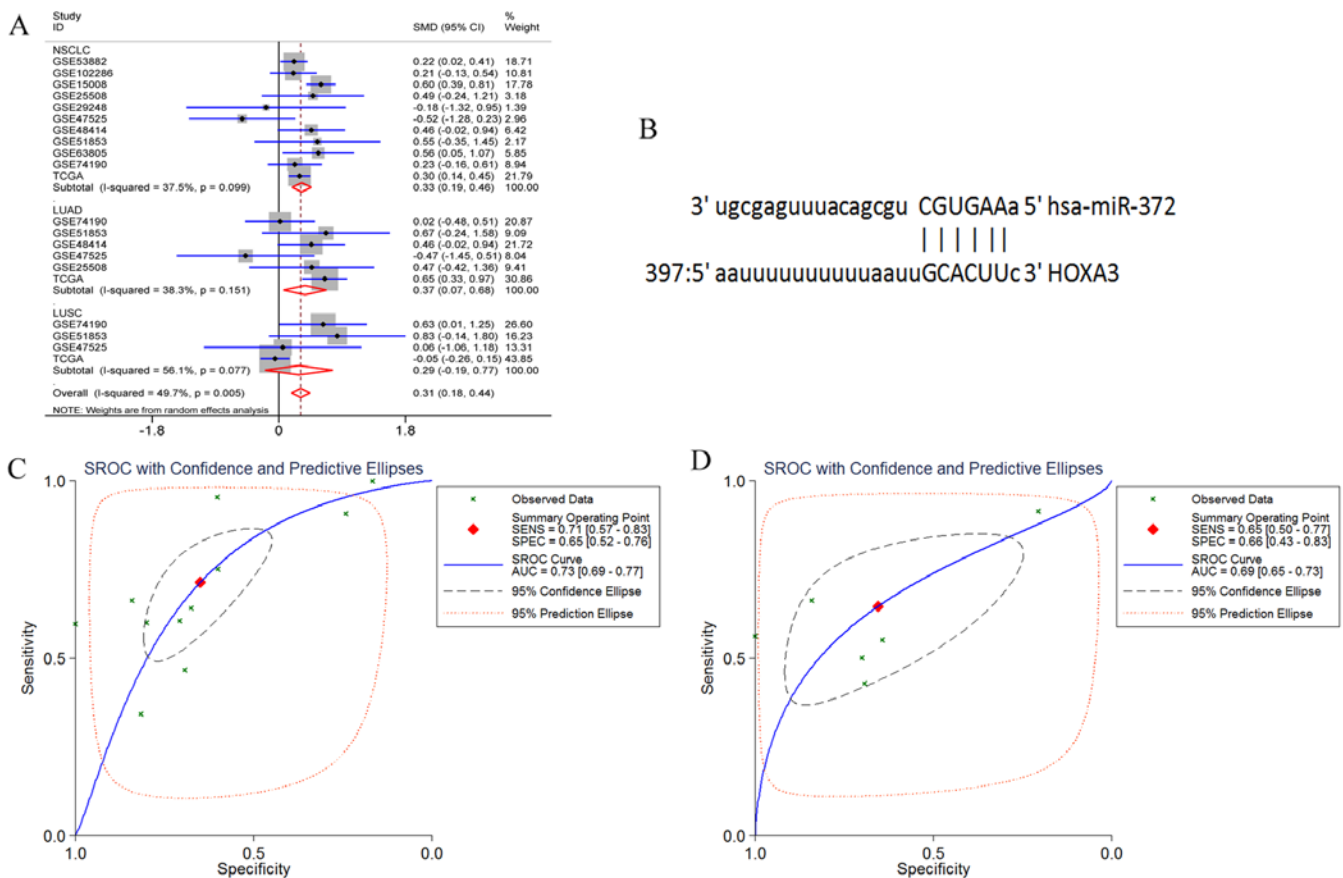

Figure 16. (A) Forest profile of SMD of miR-372-3p expression between NSCLC and normal lung tissue. (B) The complementary sequences existing between miR-372-3p and HOXA3. (C and D) The combined sROC curve for miR-372-3P expression between NSCLC and normal lung tissue; (C) NSCLC and (D) LUAD. HOXA3, homeobox A3; NSCLC, non-small cell lung cancer; LUAD, lung adenocarcinoma.

expression and *HOXA3* may carry out its function through the targeted upregulation of miR-372-3p. However, this hypothesis needs to be validated using various experiments.

In conclusion, combined with the RT-qPCR detection results and data from the TCGA and GEO databases, we confirmed that *HOXA3* expression was downregulated in LUAD tissues

Table IX. Top 10 with combined score co-expression correlation by STRING 10.5 of homeobox A3 (HOXA3) co-expression genes in lung adenocarcinoma.

#Node1	Node2	Node1 STRING internal ID	Homology	Co-expression	Experimentally determined interaction	Automated text mining	Combined score
STX2	SNAP25	1858001	0	0.093	0.939	0.905	0.998
ARRB1	MAPK1	1860799	0	0	0.43	0.658	0.978
EGFR	MAPK1	1846445	0.632	0	0.503	0.932	0.965
MALT1	CARD10	1850132	0	0	0.115	0.63	0.964
COL6A1	COL1A1	1854318	0.617	0.504	0	0.49	0.957
PDE10A	ADCY6	1862089	0	0.207	0.169	0.384	0.954
ARRB1	EGFR	1860799	0	0	0.165	0.416	0.947
EGFR	CFTR	1846445	0	0	0	0.445	0.942
EGFR	ERBB3	1846445	0.921	0.05	0.36	0.956	0.938
TGFB2	THBS1	1854475	0	0.046	0	0.364	0.934
STX2	SNAP25	1858001	0	0.093	0.939	0.905	0.998
ARRB1	MAPK1	1860799	0	0	0.43	0.658	0.978
EGFR	MAPK1	1846445	0.632	0	0.503	0.932	0.965
MALT1	CARD10	1850132	0	0	0.115	0.63	0.964
COL6A1	COL1A1	1854318	0.617	0.504	0	0.49	0.957

Table X. Top 10 with combined co-expression score that the protein-protein interaction (PPI) of homeobox A3 (HOXA3) co-expression gene intersection in lung adenocarcinoma enriched in significant signalling pathways.

#Node1	Node2	Node1 STRING internal ID	Homology	Co-expression	Experimentally determined interaction	Automated text mining	Combined score
EGFR	MAPK1	1846445	0.632	0	0.503	0.932	0.965
COL6A1	COL1A1	1854318	0.617	0.504	0	0.49	0.957
MYLK	MAPK1	1853981	0.636	0	0	0.711	0.925
LAMA3	LAMA4	1850649	0.804	0	0	0.115	0.901
PDGFD	EGFR	1858075	0	0	0	0.49	0.893
EGFR	TNC	1846445	0	0	0.36	0.72	0.813
THBS1	COL1A1	1844779	0	0.1	0.324	0.463	0.645
TNC	MAPK1	1845696	0	0	0	0.576	0.576
TNC	THBS1	1845696	0	0.052	0	0.533	0.538
FLNC	MAPK1	1850897	0	0	0.066	0.475	0.49
AKT3	MAPK1	1845421	0.65	0.134	0.292	0.576	0.486
EGFR	THBS1	1846445	0	0	0	0.457	0.457
COL6A1	TNC	1854318	0	0.055	0	0.424	0.432
TNC	COL1A1	1845696	0	0.1	0	0.369	0.408
EGFR	MAPK1	1846445	0.632	0	0.503	0.932	0.965

and exhibited a certain level of genetic alteration. The functions of downregulated *HOXA3* in tumour progression and a poor prognosis of patients with LUAD may be associated with increases in the methylation level. Furthermore, *HOXA3* may collaborate with co-expression genes, such as *TNC* and *COL1A1*, to regulate the focal adhesion and ECM-receptor interaction signalling pathways together or upregulate miR-372-3p to promote its carcinogenesis function. These study results provide true and reliable experimental data and rigorous

molecular theories for further studies on the molecular mechanisms of *HOXA3* in LUAD.

Funding

No funding was received.

Availability of data and materials

The datasets used and/or analyzed during the current study are available from the corresponding authors on reasonable request.

Authors' contributions

BLG collected data from public datasets and analyzed the data and performed the statistical analysis. RQH and YZ collected the clinical samples and performed in-house RT-qPCR experiments. RQH and GC participated in the conception and design of the study and in language modification. BLG and RQH drafted the manuscript and analyzed the GO and KEGG terms. DMW and XHH conceived and designed the study and assisted in the drafting of the manuscript. All authors have read and approved the final manuscript.

Ethics approval and consent to participate

This research programme was approved by the Ethics Committee of the First Affiliated Hospital of Guangxi Medical University. All participants signed informed consent forms.

Patient consent for publication

Not applicable.

Competing interests

The authors declare that they have no competing interests.

References

1. Siegel RL, Miller KD and Jemal A: Cancer Statistics, 2017. CA Cancer J Clin 67: 7-30, 2017.
2. Cancer UK: Lung cancer mortality statistics. 2014.
3. Chen W, Zheng R, Baade PD, Zhang S, Zeng H, Bray F, Jemal A, Yu XQ and He J: Cancer statistics in China, 2015. CA Cancer J Clin 66: 115-132, 2016.
4. Miller KD, Siegel RL, Lin CC, Mariotto AB, Kramer JL, Rowland JH, Stein KD, Alteri R and Jemal A: Cancer treatment and survivorship statistics, 2016. CA Cancer J Clin 66: 271-289, 2016.
5. Govindan R, Page N, Morgensztern D, Read W, Tierney R, Vlahiotis A, Spitznagel EL and Piccirillo J: Changing epidemiology of small-cell lung cancer in the United States over the last 30 years: Analysis of the surveillance, epidemiologic, and end results database. J Clin Oncol 24: 4539-4544, 2006.
6. O'Brien TD, Jia P, Caporaso NE, Landi MT and Zhao Z: Weak sharing of genetic association signals in three lung cancer subtypes: Evidence at the SNP, gene, regulation, and pathway levels. Genome Med 10: 16, 2018.
7. Abraham C, Garsa A, Badiyan SN, Drzymala R, Yang D, DeWees T, Tsien C, Dowling JL, Rich KM, Chicoine MR, *et al*: Internal dose escalation is associated with increased local control for non-small cell lung cancer (NSCLC) brain metastases treated with stereotactic radiosurgery (SRS). Adv Radiat Oncol 3: 146-153, 2017.
8. Fernandes P, Lareiro S, Vouga L, Guerra M and Miranda J: Uniportal video-assisted thorascoscopic surgery - The new paradigm in the surgical treatment of lung cancer. Rev Port Cir Cardiotorac Vasc 24: 127, 2017.
9. Jean F, Tomasini P and Barlesi F: Atezolizumab: Feasible second-line therapy for patients with non-small cell lung cancer? A review of efficacy, safety and place in therapy. Ther Adv Med Oncol 9: 769-779, 2017.
10. Jiang Q, Xie M, He M, Yan F, Zhang X and Yu S: Anti-PD-1/PD-L1 antibodies versus docetaxel in patients with previously treated non-small-cell lung cancer. Oncotarget 9: 7672-7683, 2017.
11. Byrne M, Martinez P and Morris V: Evolution of a pentameral body plan was not linked to translocation of anterior Hox genes: The echinoderm HOX cluster revisited. Evol Dev 18: 137-143, 2016.
12. Kim HS, Kim BM, Lee BY, Souissi S, Park HG and Lee JS: Identification of Hox genes and rearrangements within the single homeobox (Hox) cluster (192.8 kb) of the cyclopoid copepod (*Paracyclopina nana*). J Exp Zoolog B Mol Dev Evol 326: 105-109, 2016.
13. Schiemann SM, Martín-Durán JM, Børve A, Vellutini BC, Passamaneck YJ and Hejnol A: Clustered brachiopod Hox genes are not expressed collinearly and are associated with lophotrochozoan novelties. Proc Natl Acad Sci USA 114: E1913-E1922, 2017.
14. Wang X, Bu J, Liu X, Wang W, Mai W, Lv B, Zou J, Mo X, Li X, Wang J, *et al*: miR-133b suppresses metastasis by targeting HOXA9 in human colorectal cancer. Oncotarget 8: 63935-63948, 2017.
15. Wang K, Jin J, Ma T and Zhai H: MiR-139-5p inhibits the tumorigenesis and progression of oral squamous carcinoma cells by targeting HOXA9. J Cell Mol Med 21: 3730-3740, 2017.
16. Fu Z, Chen C, Zhou Q, Wang Y, Zhao Y, Zhao X, Li W, Zheng S, Ye H, Wang L, *et al*: LncRNA HOTTIP modulates cancer stem cell properties in human pancreatic cancer by regulating HOXA9. Cancer Lett 410: 68-81, 2017.
17. Chen S, Yu J, Lv X and Zhang L: HOXA9 is critical in the proliferation, differentiation, and malignancy of leukaemia cells both in vitro and in vivo. Cell Biochem Funct 35: 433-440, 2017.
18. Sang Y, Zhou F, Wang D, Bi X, Liu X, Hao Z, Li Q and Zhang W: Up-regulation of long non-coding HOTTIP functions as an oncogene by regulating HOXA13 in non-small cell lung cancer. Am J Transl Res 8: 2022-2032, 2016.
19. Daugaard I, Dominguez D, Kjeldsen TE, Kristensen LS, Hager H, Wojdacz TK and Hansen LL: Identification and validation of candidate epigenetic biomarkers in lung adenocarcinoma. Sci Rep 6: 35807, 2016.
20. Zhang Y, Chen WJ, Gan TQ, Zhang XL, Xie ZC, Ye ZH, Deng Y, Wang ZF, Cai KT, Li SK, *et al*: Clinical significance and effect of lncRNA HOXA11-AS in NSCLC: A study based on bioinformatics, in vitro and in vivo verification. Sci Rep 7: 5567, 2017.
21. Tang RX, Chen WJ, He RQ, Zeng JH, Liang L, Li SK, Ma J, Luo DZ and Chen G: Identification of a RNA-Seq based prognostic signature with five lncRNAs for lung squamous cell carcinoma. Oncotarget 8: 50761-50773, 2017.
22. Li Z, Xie Y, Zhong T, Zhang X, Dang Y, Gan T and Chen G: Expression and clinical contribution of MRGD mRNA in non-small cell lung cancers. J BUON 20: 1101-1106, 2015.
23. Muraoka T, Soh J, Toyooka S, Aoe K, Fujimoto N, Hashida S, Maki Y, Tanaka N, Shien K, Furukawa M, *et al*: The degree of microRNA-34b/c methylation in serum-circulating DNA is associated with malignant pleural mesothelioma. Lung Cancer 82: 485-490, 2013.
24. Singh J, Batish VK and Grover S: Simultaneous detection of Listeria monocytogenes and Salmonella spp. in dairy products using real time PCR-melt curve analysis. J Food Sci Technol 49: 234-239, 2012.
25. Xu D, Yang Z, Zhang D, Wu W, Guo Y, Chen Q, Xu D and Cui W: Rapid detection of immunoglobulin heavy chain gene rearrangement by PCR and melting curve analysis using combined FR2 and FR3 primers. Diagn Pathol 10: 140, 2015.
26. Zaghloul H, El Morsi AA, Soweha HE, Elsayed A, Seif S and El-Sharawy H: A simple real-time polymerase chain reaction assay using SYBR Green for hepatitis C virus genotyping. Arch Virol 162: 57-61, 2017.
27. Livak KJ and Schmittgen TD: Analysis of relative gene expression data using real-time quantitative PCR and the 2(-Delta Delta C(T)) method. Methods 25: 402-408, 2001.
28. Tang R, Liang L, Luo D, Feng Z, Huang Q, He R, Gan T, Yang L and Chen G: Downregulation of miR-30a is associated with poor prognosis in lung cancer. Med Sci Monit 21: 2514-2520, 2015.
29. Ren F, Ding H, Huang S, Wang H, Wu M, Luo D, Dang Y, Yang L and Chen G: Expression and clinicopathological significance of miR-193a-3p and its potential target astrocyte elevated gene-1 in non-small lung cancer tissues. Cancer Cell Int 15: 80, 2015.

30. Zhang X, Liu G, Ding L, Jiang T, Shao S, Gao Y and Lu Y: HOXA3 promotes tumor growth of human colon cancer through activating EGFR/Ras/Raf/MEK/ERK signaling pathway. J Cell Biochem 119: 2864-2874, 2018.

31. Shen ZH, Zhao KM and Du T: HOXA10 promotes nasopharyngeal carcinoma cell proliferation and invasion via inducing the expression of ZIC2. Eur Rev Med Pharmacol Sci 21: 945-952, 2017.

32. Kuasne H, Cólus IM, Busso AF, Hernandez-Vargas H, Barros-Filho MC, Marchi FA, Scapulatempo-Neto C, Faria EF, Lopes A, Guimarães GC, et al: Genome-wide methylation and transcriptome analysis in penile carcinoma: Uncovering new molecular markers. Clin Epigenetics 7: 46, 2015.

33. Zhang X, Liu G, Ding L, Jiang T, Shao S, Gao Y and Lu Y: HOXA3 promotes tumor growth of human colon cancer through activating EGFR/Ras/Raf/MEK/ERK signaling pathway. J Cell Biochem 119: 2864-2874, 2018.

34. Zhang YW, Zheng Y, Wang JZ, Lu XX, Wang Z, Chen LB, Guan XX and Tong JD: Integrated analysis of DNA methylation and mRNA expression profiling reveals candidate genes associated with cisplatin resistance in non-small cell lung cancer. Epigenetics 9: 896-909, 2014.

35. Jin X, Liu X, Li X and Guan Y: Integrated analysis of DNA methylation and mRNA expression profiles data to identify key Genes in lung adenocarcinoma. Biomed Res Int 2016: 4369431, 2016.

36. Tai YL, Chen LC and Shen TL: Emerging roles of focal adhesion kinase in cancer. Biomed Res Int 2015: 690690, 2015.

37. Min A, Zhu C, Wang J, Peng S, Shuai C, Gao S, Tang Z and Su T: Focal adhesion kinase knockdown in carcinoma-associated fibroblasts inhibits oral squamous cell carcinoma metastasis via downregulating MCP-1/CCL2 expression. J Biochem Mol Toxicol 29: 70-76, 2015.

38. Eke I and Cordes N: Focal adhesion signaling and therapy resistance in cancer. Semin Cancer Biol 31: 65-75, 2015.

39. Zhou B, Wang GZ, Wen ZS, Zhou YC, Huang YC, Chen Y and Zhou GB: Somatic mutations and splicing variants of focal adhesion kinase in non-small cell lung cancer. J Natl Cancer Inst 110: 195-204, 2017.

40. Tang KJ, Constanzo JD, Venkateswaran N, Melegari M, Ilcheva M, Morales JC, Skoulidis F, Heymach JV, Boothman DA and Scaglioni PP: Focal adhesion kinase regulates the DNA damage response and its inhibition radiosensitizes mutant KRAS lung cancer. Clin Cancer Res 22: 5851-5863, 2016.

41. Zhang HJ, Tao J, Sheng L, Hu X, Rong RM, Xu M and Zhu TY: Twist2 promotes kidney cancer cell proliferation and invasion by regulating ITGA6 and CD44 expression in the ECM-receptor interaction pathway. Onco Targets Ther 9: 1801-1812, 2016.

42. Zhang H, Ye J, Weng X, Liu F, He L, Zhou D and Liu Y: Comparative transcriptome analysis reveals that the extracellular matrix receptor interaction contributes to the venous metastases of hepatocellular carcinoma. Cancer Genet 208: 482-491, 2015.

43. Lv M and Wang L: Comprehensive analysis of genes, pathways, and TFs in nonsmoking Taiwan females with lung cancer. Exp Lung Res 41: 74-83, 2015.

44. GE ZH, Cheng QS, LI WM, Feng Z, Wen MM, Wang WC, Zhang ZP: Expression of TNC in NSCLC and its clinical significance. Xiandai Shengwu Yixue Jinzhan 31: 6103-6106, 2014 (In Chinese).

45. Gocheva V, Naba A, Bhutkar A, Guardia T, Miller KM, Li CM, Dayton TL, Sanchez-Rivera FJ, Kim-Kiselak C, Jailkhani N, et al: Quantitative proteomics identify Tenascin-C as a promoter of lung cancer progression and contributor to a signature prognostic of patient survival. Proc Natl Acad Sci USA 114: E5625-E5634, 2017.

46. Edlund K, Lindskog C, Saito A, Berglund A, Pontén F, Göransson-Kultima H, Isaksson A, Jirström K, Planck M, Johansson L, et al: CD99 is a novel prognostic stromal marker in non-small cell lung cancer. Int J Cancer 131: 2264-2273, 2012.

47. Oleksiewicz U, Liloglou T, Tasopoulou KM, Daskoulidou N, Gosney JR, Field JK and Xinarianos G: COL1A1, PRPF40A, and UCP2 correlate with hypoxia markers in non-small cell lung cancer. J Cancer Res Clin Oncol 143: 1133-1141, 2017.

48. Wang Q, Liu S, Zhao X, Wang Y, Tian D and Jiang W: MiR-372-3p promotes cell growth and metastasis by targeting FGF9 in lung squamous cell carcinoma. Cancer Med 6: 1323-1330, 2017.

49. Syring I, Bartels J, Holdenrieder S, Kristiansen G, Müller SC and Ellinger J: Circulating serum miRNA (miR-367-3p, miR-371a-3p, miR-372-3p and miR-373-3p) as biomarkers in patients with testicular germ cell cancer. J Urol 193: 331-337, 2015.